Structure-Based Lead Optimization and Biological Evaluation of BAX Direct Activators as Novel Potential Anticancer Agents

Mariano Stornaiuolo,*[,†] Giuseppe La Regina,[‡] Sara Passacantilli,[‡] Gianluca Grassia,[†] Antonio Coluccia,[‡] Valeria La Pietra,[†] Mariateresa Giustiniano,[†] Hilde Cassese,[†] Salvatore Di Maro,[†] Diego Brancaccio,[†] Sabrina Taliani,[§] Armando Ialenti,[†] Romano Silvestri,[‡] Claudia Martini,[§] Ettore Novellino,[†] and Luciana Marinelli*[,†]

[†]Dipartimento di Farmacia, Università di Napoli "Federico II", via D. Montesano 49, 80131 Naples, Italy

[‡]Istituto Pasteur-Fondazione Cenci Bolognetti, Dipartimento di Chimica e Tecnologie del Farmaco, Sapienza Università di Roma, Piazzale Aldo Moro 5, I-00185 Roma, Italy

[§]Dipartimento di Farmacia, Università di Pisa, Via Bonanno 6, 56126 Pisa, Italy

ABSTRACT: The first direct activator of BAX, a pro- apoptotic member of the BCL-2 family, has been recently identified. Herein, a structure-based lead optimization turned out into a small series of analogues, where 8 is the most potent compound published so far. 8 was used as pharmacological tool to ascertain, for the first time, the anticancer potential of BAX direct activators and the obtained results would suggest that BAX direct activators are potential future anticancer drugs rather than venoms.

The lack of efficacy of marketed anticancer drugs is due, at least in part, to the tumor ability to escape apoptosis. Thus, novel medicines, designed to activate the cell death machinery, have recently appeared as innovative anticancer drugs.[1] In vertebrates, there are two major routes leading to apoptosis, the activation of death receptors or the mitochondrial outer membrane permeabilization (MOMP),[2] which allows proteins such cytochrome C (cyt-C) to orchestrate the activation of caspases and in turn the cell dismantling. MOMP is finely regulated by a complex play among BCL-2 family members, which makes these proteins prime targets for therapeutic intervention in cancer.[3] Within this family, three main subgroups are known: (a) the antiapoptotic members (e.g., BCL-2, BCL-X_L, MCL-1, A1), (b) the pro-apoptotic members (e.g., BAK and BAX),[4] and (c) the pro-apoptotic BH3-only proteins[5] (e.g., BID, BIM, PUMA, BAD, NOXA).[6] The evidence that, in cancer cells, the neutralization of antiapoptotic BCL-2 proteins unleashes mitochondrial apoptosis and that high levels of antiapoptotic BCL-2 family members are often associated with tumor resistance, led to a massive structure-aided medicinal chemistry effort which culminated in the development of BH3 mimetics, such as the 4-[4-[[2-(4-chlorophenyl)phenyl]methyl]piperazin-1-yl]-*N*-[4-[[(2*R*)-4-(dimethylamino)-1-phenylsulfanylbutan-2-yl]amino]-3-nitrophenyl]sulfonylbenzamide (ABT737),[7] (4-[4-[[2-(4-chlorophenyl)-5,5-dimethylcyclohexen-1-yl]methyl]piperazin-1-yl]-*N*-[4-[[(2*R*)-4-morpholin-4-yl-1-phenylsulfanylbutan-2-yl]-amino]-3-(trifluoromethylsulfonyl)phenyl]sulfonylbenzamide (Navitoclax or ABT263),[8] or the newly developed (4-[4-[[2-(4-chlorophenyl)-4,4-dimethylcyclohexen-1-yl]methyl]piperazin-1-yl]-*N*-[3-nitro-4-(oxan-4-ylmethylamino)phenyl]sulfonyl-2-(1*H*-pyrrolo[2,3-*b*]pyridin-5-yloxy)benzamide (ABT199).[9] However, despite their promises, some of these drugs, which are in diverse clinical phases for human tumors treatment, were shown to cause side effects (thrombocytopenia, tumor lysis syndrome,[10] etc.) or to be less efficient on specific kind of tumors, like MCL-1 overexpressing ones. Thus, in the search for novel small molecules as alternative modulators of cell death, the recent discovery of a new BAX activation site (also named trigger site or rear site)[11] offered a thrilling opportunity to develop a novel class of alternative apoptosis activators. As such, the identification of the first, and so far still unique, small molecule 1[12] (BAM-7) (Figure 1) as BAX direct activator surely represents a milestone in the field. However, the results so far published do not allow the understanding of BAX requirements for small ligands recognition and binding; in fact, structure−activity relationship (SAR) studies were just focused on derivatizations at the phenylhydrazono and phenylthiazole

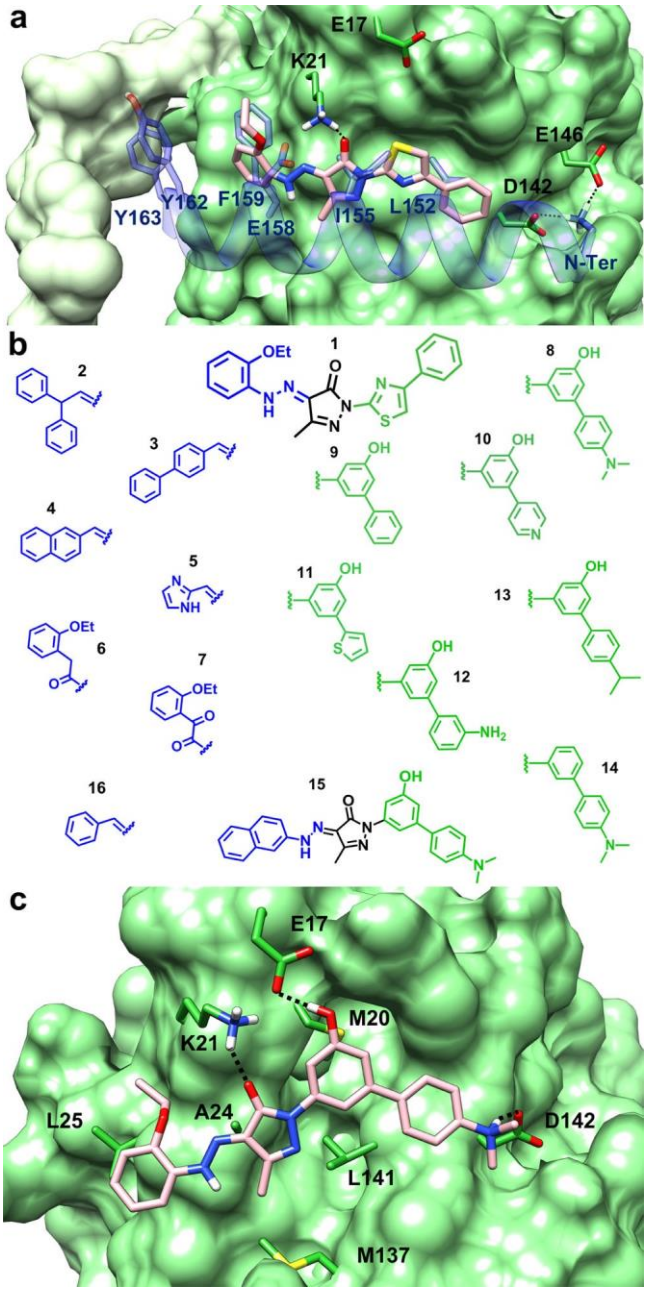

Figure 1. Design strategy. (a) Docked structure of 1 (pink) at the BAX rear site (green surface). Interacting protein residues are highlighted as green sticks, the α1−α2 loop is depicted as light green surface. BIM−BH3 helix bound to the BAX rear site (PDB code: 2K7W) is colored in transparent blue, with interacting residues depicted as blue sticks. (b) Representation of the rebranching approach. (c) Binding mode of 8 within BAX rear site.

side groups of 1[12] with small groups with no improvement of activity.[12] Moreover, neither the in vitro or in vivo anticancer property besides apoptotic effects on MEF cells, nor the capability of this lead to discriminate between cancer cells and healthy cells was assessed.

Herein, we report the results of our lead optimization program, which culminated in the discovery of 1-(4′-(dimethylamino)-5-hydroxy-[1,1′-biphenyl]-3-yl)-4-(2-(2-ethoxyphenyl)hydrazono)-3-methyl-1*H*-pyrazol-5(4*H*)-one (8 or Bax targeting compound-8, BTC-8), which directly binds to BAX and, in tumor cell lines, induces MOMP with an EC_{50} 1 order of magnitude lower than that exhibited by 1[12] in cultured HuH7 cells. As such, it is the most active, low molecular weight, direct activator of BAX reported in the published literature. To reveal the anticancer potential of 8, as an illustrative example of BAX direct activator, the latter was tested in a small panel of tumor cell lines and on an healthy cell line, providing encouraging results, which in turn prompted us to test 8 in a mouse model of lung carcinoma. The in vivo preliminary study would suggest that BAX direct activators are potential future anticancer drugs rather than venoms.

RESULTS AND DISCUSSION

Design Strategy. The three-dimensional superimposition of BAX, alone (inactive state)[13] and with BIM−BH3 helix (active state) bound in the "rear site"[11] clearly revealed that, upon BIM binding, significant changes took place in the α1−α2 loop, which moves from a closed to an open conformation. Similar changes were observed upon 1 binding.[12] As the first step of our lead optimization protocol, docking experiments were performed, by means of Glide,[14,15] in order to reproduce the 1 binding mode,[12] which was then overlapped onto that of BIM peptide. As shown in Figure 1a, the strongest interaction was observed between the carbonyl group of 1 pyrazolone core and the BAX K21, a key residue which interacts with BIM as well (see Figure 1a, charge−charge interaction with BIM E158). Notably, the ethoxyphenyl group of 1 lays adjacent to a presumed hinge site for loop opening upon initiation of BAX activation and well overlaps onto BIM F159. However, as shown in Figure 1a, the BIM−BH3 helix is much longer if, compared to 1, holding five further amino acids next to F159, (e.g., Y162 and Y163). On the opposite side, the phenylthiazole portion of 1 well fitted on BIM L152 and I155, although lacking the terminal amino group, that as in the case of BIM, engages charge reinforced hydrogen bonds with BAX D142 and E146, respectively. On the basis of these premises, we planned lead optimization studies of 1 aimed at understanding the BAX requirements and hopefully at improving the binding affinity. Given the importance of the pyrazolone core, it was retained while a rebranching approach was accomplished in the attempt to better mimic the essential features of the physiological activator (BIM BH3 only protein). Thus, as shown in Figure 1b, a number of different moieties were considered. Basically, in the replacement of the 2-ethoxyphenyl-hydrazono group, two considerations were taken into account: (i) substitution of hydrazone bridge with other spacer groups, for synthetic reasons, and (ii) substitution of the ethoxyphenyl with bulkier aromatic moieties (see compounds 2−7, and 15−16), in the attempt to approach the region occupied by BIM Tyr residues (see Figure 1S, Supporting Information (SI)), which abut the hinge site for α1−α2 loop opening. Analogously, for the replacement of the phenylthiazole group, the substitutions were planned based on the following considerations: (i) neither the N nor the S of the thiazole ring engaged interactions with BAX, so that the thiazole ring could, in principle, be replaceable by other aromatic systems such as phenyl ring, which can be easily substituted with the aim to establish further interactions with other BAX residues (e.g., E17), (ii) the *para* position of the biphenyl moiety is in proximity of D142 that together with E146 seizes the BIM amino terminal group (Figure 1a). Thus, we inserted an exocyclic or endocyclic basic group at the terminal phenyl ring (8, 12, and 10, respectively). Compounds 9 and 13 were synthesized as negative control to test the importance of the *N*,*N*-dimethylamino group. Compound 14

Scheme 1. Synthesis of Compounds 2−7 and 16[a]

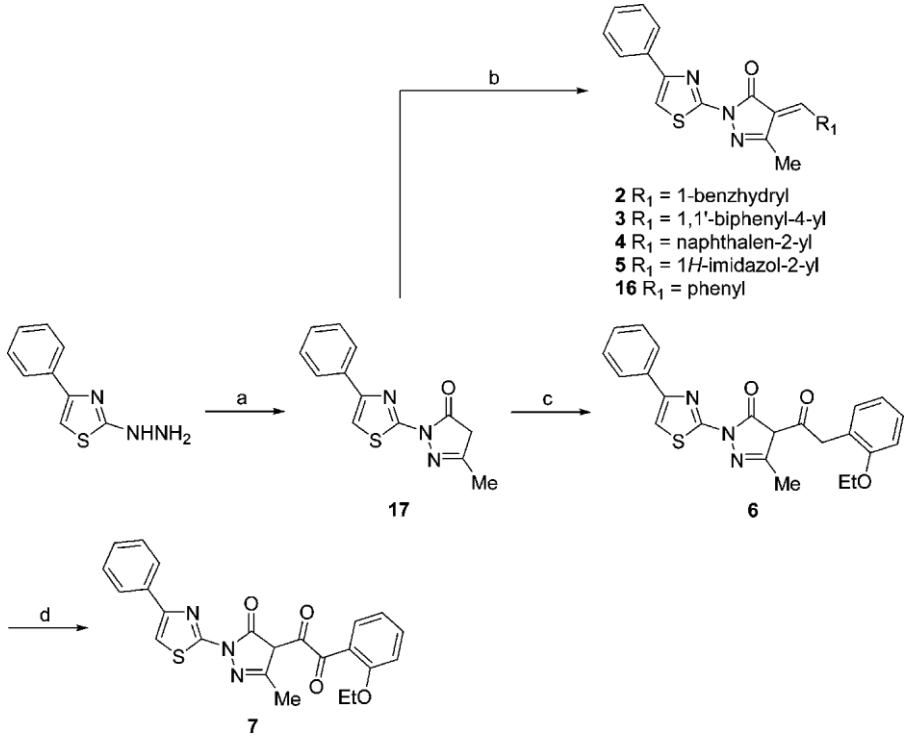

[a]Reagents and reaction conditions: (a) ethyl acetoacetate, acetic acid, reflux temperature, 3 h, 62%; (b) appropriate benzaldehyde, piperidine, anhydrous ethanol, reflux temperature, 3 h, 28−61%; (c) (i) potassium *tert*-butoxide, anhydrous tetrahydrofuran, −40 °C, 1 h, (ii) 2-(2-ethoxyphenyl)acetyl chloride, 25 °C, 1 h, 74%; (d) potassium permanganate, catalytic sulfuric acid, acetone, reflux temperature, 5%.

was synthesized as negative control to test the importance of the hydroxyl group on the biphenyl moiety. Finally, 11 was conceived as a replacement of the 5−6 thiazole-phenyl system with a 6−5-phenyl-thiazole one.

CHEMISTRY

Synthesis of compounds 2−16 are depicted in Schemes 1−3. Compounds 2−5 and 16 were prepared by reacting the 5-methyl-2-(4-phenylthiazol-2-yl)-2,4-dihydro-3*H*-pyrazol-3-one (17), obtained by treatment of 2-hydrazinyl-4-phenylthiazole with ethyl acetoacetate in acetic acid at reflux temperature for 3 h, with the appropriate benzaldehyde in the presence of piperidine in boiling ethanol for 4 h (Scheme 1). Reaction of compound 17 with 2-(2-ethoxyphenyl)acetyl chloride in the presence of potassium *tert*-butoxide in anhydrous tetrahydrofuran at 0 °C for 1 h furnished the derivative 6, which was converted into the corresponding dione 7 by oxidation with potassium permanganate in the presence of a catalytic amount of sulfuric acid in acetone at reflux temperature for 12 h. Compounds 8, 12, and 15 were synthesized starting from the 2-(3-bromo-5-hydroxyphenyl)-5-methyl-2,4-dihydro-3*H*-pyrazol-3-one (19), which was treated with 2-ethoxybenzenediazonium chloride or naphthalene-2-diazonium chloride in the presence of sodium acetate in ethanol at 0 °C for 2 h and then coupled with the appropriate boronic acid in the presence of sodium carbonate and Pd catalyst in tetrahydrofuran at reflux temperature for 90 min under Ar stream (Scheme 2). Analogously, treatment of compound 19 with the appropriate boronic acid and subsequent reaction with 2-ethoxybenzenediazonium chloride gave derivatives 9, 11, and 13. Compounds 22−24 were prepared as above-reported, starting from the 3-bromo-5-hydrazinylphenol hydrochloride (18), obtained by reaction of 3-bromo-5-nitrophenol with tin(II) chloride dihydrate in boiling ethyl acetate for 3 h, treatment with sodium nitrite and 37% HCl at 0 °C for 20 min, and final reduction with tin(II) chloride dihydrate at 0 °C for 20 min. Derivatives 10 and 14 were obtained similarly to 8, starting from pyrazolones 29 and 30, respectively (Scheme 3). Derivatives 29 and 30 were prepared as above-reported, by treatment of 3-bromo-5-nitrophenol with the appropriate boronic acid, conversion into the corresponding phenylhydrazine derivative, and final cyclization with ethyl acetoacetate.

Biological Results. *In Vitro BAX Affinity, Selectivity Profile, and SAR Rationalization.* Affinities of candidate compounds for recombinant BCl-2 family members were measured in vitro by fluorescence polarization assay (FPA). GST tagged full length BAX, untagged BCL-2, and BCL-X_L show nanomolar affinity for FITC-BIM (K_i values of 200, 132, and 794 nM, respectively) (Figure 2S, SI), in line with data previously reported.[11,12] The ability of 1−15 to displace bound FITC-BIM was used to calculate their K_i for each of the three proteins (Figure 2 and Table 1). As previously reported, 1 is selective on BAX over BCL-X_L (Figure 2 and Table 1). It displays, however, affinity for BCl-2 despite this being somehow slightly lower than the one for BAX (K_i values of 3.0 and 1.1 μM, respectively).

In the range of concentration tested, the new compounds show either higher affinity for BCl-2 over BAX and BCL-X_L (compounds 2 and 5), higher affinity for both BCl-2 and BCL-X_L over BAX (compounds 3−5), and similar affinities for the three proteins (compounds 16) or for none of them (compounds 6−7) (Table 1).

Scheme 2. Synthesis of Compounds 8, 9, 11−13, and 15[a]

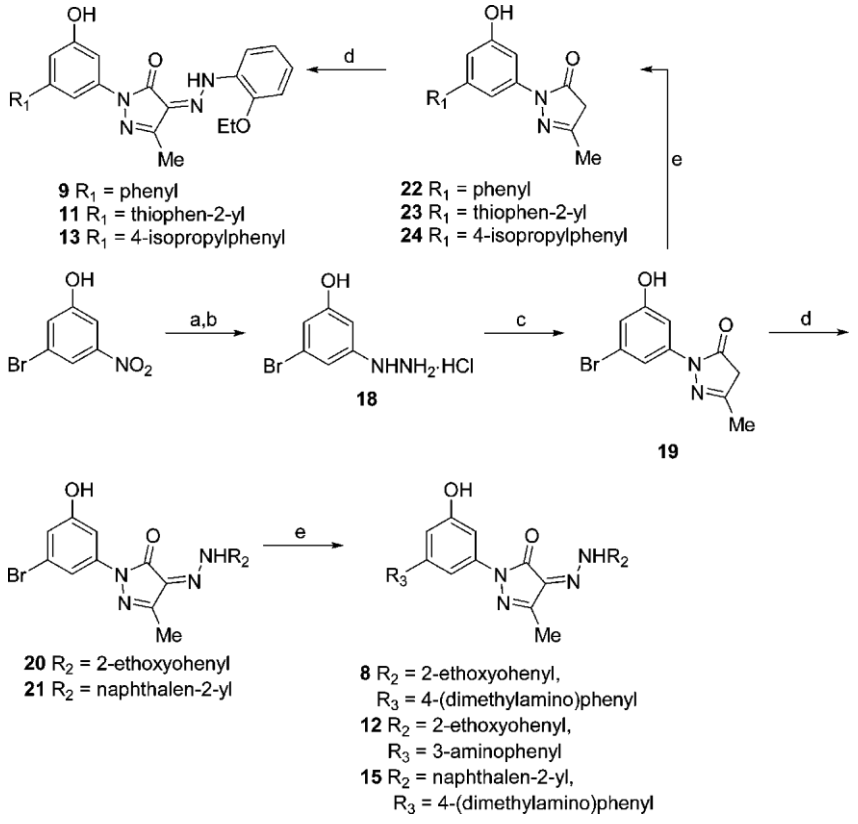

[a]Reagents and reaction conditions: (a) tin(II) chloride dihydrate, ethyl acetate, reflux, 3 h; (b) (i) sodium nitrite, 37% hydrogen chloride, 0 °C, 20 min, (ii) tin(II) chloride dihydrate, 0 °C, 20 min, crude product; (c) ethyl acetoacetate, acetic acid, 80 °C, 3 h, 13%; (d) 2-ethoxybenzenediazonium chloride or naphthalene-2-diazonium chloride, sodium acetate, 96° ethanol, 0 °C, 2 h, 3−48%; (e) appropriate boronic acid, 2 M sodium carbonate, dichloro[1,1′-bis(diphenylphosphino)ferrocene]-palladium(II) dichloromethane complex (1:1), tetrahydrofuran, reflux temperature, 90 min, Ar stream, 13−66%.

Scheme 3. Synthesis of Compounds 10 and 14[a]

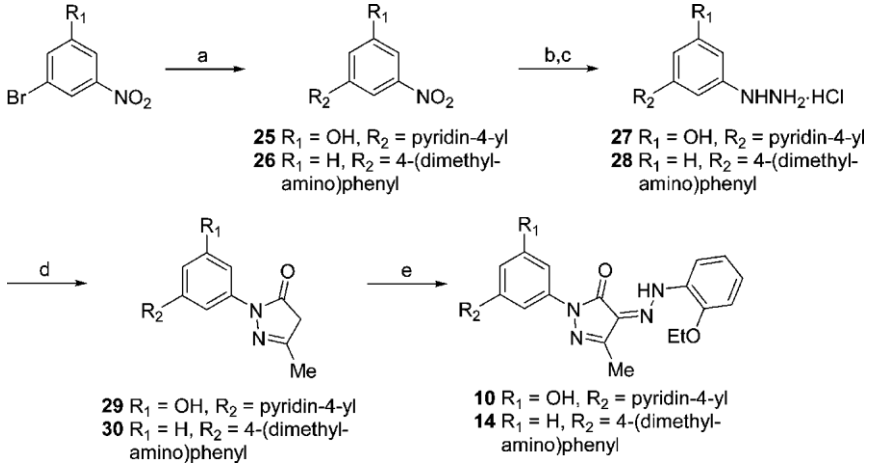

[a]Reagents and reaction conditions: (a) appropriate boronic acid, 2 M sodium carbonate, dichloro[1,1′-bis(diphenylphosphino)ferrocene]-palladium(II) dichloromethane complex (1:1), reflux temperature, 90 min, Ar stream, 14−25%; (b) tin(II) chloride dihydrate, ethyl acetate, reflux, 3 h; (c) (i) sodium nitrite, 37% hydrogen chloride, 0 °C, 20 min, (ii) tin(II) chloride dihydrate, 0 °C, 20 min, crude product; (d) ethyl acetoacetate, acetic acid, 80 °C, 3 h, 12−13%; (e) 2-ethoxybenzenediazonium chloride, sodium acetate, 96° ethanol, 0 °C, 2 h, 36−47%.

Compounds 8−10 show higher affinity for BAX over BCL-2 and BCL-X_L. Among them, 8 displays higher affinity for BAX (K_i = 0.8 μM) than 1 (K_i = 1.1 μM, Figure 2). 9 and 11 are selective for BAX, but they are somehow weaker binders than 8. 12 is specific for BAX, but its BAX affinity is lower than 8 and comparable to that of 1. 13−15 display high affinity for BAX but less specificity (Table 1) over the other two proteins.

SAR toward BAX were rationalized on the basis of the complex between 1 and BAX, which was previously obtained by a combined approach of docking and NMR experiments[12] and

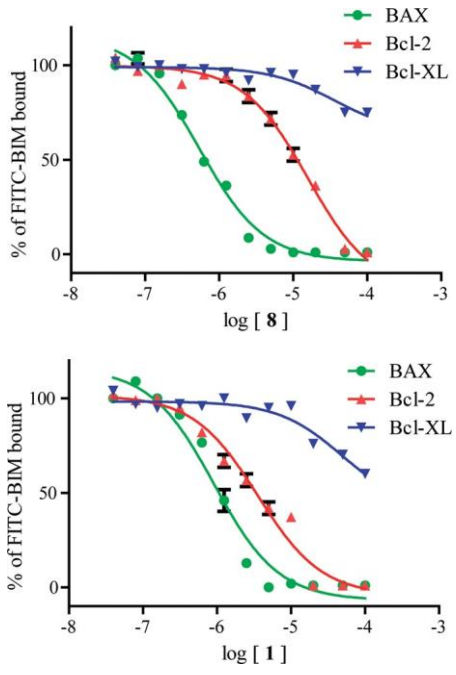

Figure 2. 8 binds BAX at BIM binding site. Competition between 8 (upper panel) or 1 (lower panel) and FITC-BIM for binding to BAX (green curve), BCL-2 (red curve), and BCL-X_L (blue curve). Mean of three experiments (SD are indicated).

Table 1. K_i (μM) of Compounds 1−15 for BAX, BCL-2, and BCL-X_L (FPA, FITC-BIM Displacement)

compd	BAX	BCL-2	BCL-X_L
1	1.1	3.0	>100
2	13.5	1.6	>100
3	12.9	1.6	3.1
4	12.6	2.0	3.4
5	15.8	2.0	6.8
6	63.1	>100	>100
7	85.1	>100	>100
8	0.8	12.0	>100
9	9.1	>100	>100
10	1.7	>100	30.9
11	30.9	>100	>100
12	1.3	>100	>100
13	1.2	1.9	15.5
14	1.3	4.2	>100
15	1	33.9	3.4
16	2.5	1.9	2.4

on the basis of docking of its analogue 8. Molecular docking of 8 within the BAX rear site resulted in a binding mode highly superimposable to that of 1 (Figure 1a,c). However, in line with the lower K_i of 8, compared to that of 1, 8 reinforces its binding to BAX surface through an H-bond with E17 by the ligand hydroxyl group and through a charge reinforced hydrogen bond with D142 coupled with hydrophobic interactions between the methyl groups and D142 carbon chain. According to the observed interactions, 9 (unsubstituted on the terminal phenyl ring) is less active than 8, 13, and 14. The importance of an amino group on the terminal phenyl ring is also proved by the affinity of 12 compared to that of 9 and by the reduced specificity of 13 compared to 8 and 12. All in all, SAR where the phenylthiazole group is replaced by other moieties clearly demonstrate that such a branch is replaceable by other aromatic systems, that if adequately decorated bring an improvement of BAX affinity. Regarding the 2-ethoxyphenylhydrazono group of 1, SAR were designed to explore: (i) bridges different from the hydrazono one and (ii) possible, fruitful hydrophobic interactions established by different aromatic moieties. Among the different bridges synthesized, just the ene one (16) seems to be well tolerated. The higher K_i of 6 and 7 seemed to be ascribable to the different geometries of ketomethylen- and diketo bridges with respect to hydrazono group, which would bring the 2-ethoxyphenyl farther from L25, with which an hydrophobic interaction was observed (Figure 1a). Although no H-bond between the ethoxy group of 1 and K21 was observed with a semiflexible docking approach, their proximity would suggest a possible interaction, which can be also the reason for the slightly lower K_i of 16 with respect to that of 1. Analogues of 1, where the phenyl moiety were replaced by a benzhydryl (2), biphenyl (3), and naphthalene (4) group, were all less active than the lead. Rationalization of the lower K_i of 2−4 is somehow difficult, as the benzhydryl, biphenyl, and naphthalene group would occupy the hinge site for loop opening, a region that undergoes to profound change upon ligand binding and activation.

Cell Viability and Apoptosis Assays. Affinities and selectivity of 1−15 measured by FPA well correlate with their potency on inducing apoptosis in MEF knock out cells. At the EC_{50} of 1, all the compounds but 6, 7, and 11 induced apoptosis in MEF wt cells (Table 2 and Table 1S, SI), while they were ineffective on

Table 2. EC_{50} (μM) Values of Apoptosis Induction of Compound 8 or 1 Treatment on the Indicated MEF Knockout Clones

compd	wt	$Bcl2^{-/-}$	$Bad^{-/-}$	$Bid^{-/-}$	$Bak^{-/-}$	$Bax^{-/-}$	$Bax^{-/-}$ $Bak^{-/-}$
1	7.7	3.2	3.5	4.0	6.0	>50	>50
8	1.1	0.6	0.8	0.7	1.3	>50	>50

MEF $BAK^{-/-}$ $BAK^{-/-}$ double knockout cells, indicating that they ultimately lead to pro-apoptotic protein activation. 1, 8−10, and 12−15 are the most effective at the concentration of 10 μM. 2−5 potencies are overall lower and partially affected by the absence of BCL-2 as well as of BID, BAD, BAK, or BAX, suggesting that, at least in MEF cells, BAX direct activation is not their main mechanism of action (Table 1S, SI). On the contrary, 1, 8−10, and 12−16 induce apoptosis independently by the absence of BCL-2, BID, and BAD, pointing to their target being located downstream in the apoptotic pathway (Figure 3, Table 2 and Table 1S, SI). 12, 13, 14, and 16 affected MEF $BAX^{-/-}$ as well as MEF $BAK^{-/-}$, indicating that they can trigger apoptosis either by BAK or by BAX. 8−10 and 15 similarly to 1 induced apoptosis in $BAK^{-/-}$ but not in $BAX^{-/-}$ knockout cells and represent, among the tested ones, the candidate compounds with the best features of selective BAX activators (Figure 3, Table 2 and Table 1S, SI). MEF cells treated with 8, the most potent compound of our series (EC_{50} of 8 on MEF-wt of 1.1 μM, EC_{50} of 1 on MEF-wt of 7.7 μM) undergo apoptotic processes, as shown by the appearance of fragmented nuclei and cell membrane blebbing. Moreover, its potency is reduced by the presence of the caspase inhibitor Ac-DEVD-CHO[16] (Figure 3), indicating that its mechanism of action involve apoptotic effectors.

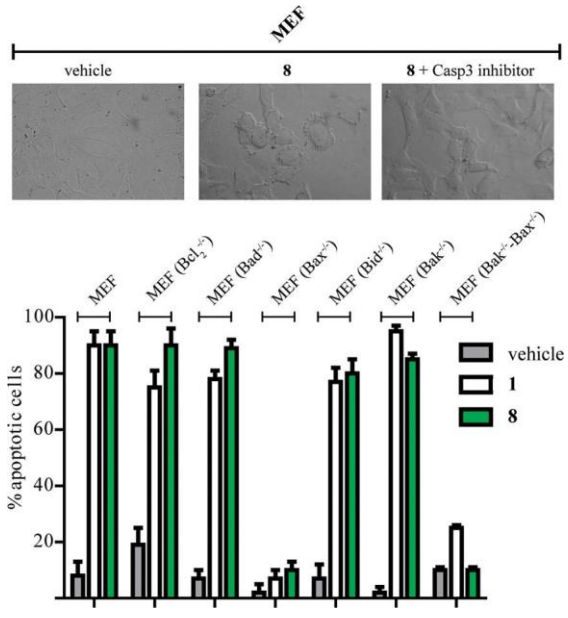

Figure 3. 8 induces apoptosis in a BAX dependent way. Effect of 8 treatment on MEF cells. Apoptotic rate of the indicated MEF clones upon 24 h of treatment with vehicle (0.1% DMSO, gray bars), 1 (15 μM, white bars), or 8 (15 μM, green bars). The photographs represent appearance of apoptotic cell membrane blebbing upon MEF treatment with 8 and its absence when 8 treatment was done in the presence of the caspase inhibitor Ac-DEVD-CHO (10 μM).

Differently from MEF cells, tumor cells overcome pro-apoptotic stimuli by overexpressing antiapoptotic proteins or by downregulating pro-apoptotic ones. We thus decided to challenge our compounds in inducing apoptosis in in vitro cultured tumor cells. Apoptosis was followed in human hepatoma HuH7 cells, which express wt BAX, a high level of BCL-2 but a low level of caspase 3,[17] the final effector of the apoptotic cascade. Under apoptotic stimuli, they survive for longer time than other tumor cells and, thus, they represent an ideal platform to look exclusively at the early events of the apoptotic process.

Apoptosis was followed in HuH7 by measuring MOMP, which inhibits mitochondrial accumulation of the fluorescent probe Mitotracker Red. Among the tested compounds, 8 was the most potent in affecting probe accumulation (Figure 4 and Figure 3S, SI). Other compounds of the series (e.g., 2 and 3) affected mitochondrial potential only after 72 h of treatment, in line with a reduced affinity for BAX but an increased affinity for BCL-2 or BCL-X_L or both (Table 1 and Figure 3S, SI). While 1 and 8 affected the cultures similarly at 10 μM, 8 induced a stronger reduction in probe accumulation at 1 μM (Figure 4a). The higher potency of 8 over 1 was quantified by a dose response curve revealing the EC_{50} of 1 and 8 in cultured HuH7 cells to be 8.2 μM and 700 nM, respectively (Figure 4b and Table 2S, SI). Similarly to 1, 8 induces a conformational change in BAX that exposes an epitope recognized by the anti-BAX 6A7 antibody,[12] specific for the activated form of the protein (Figure 4S, SI). As expected from a BAX direct activator, 8 was able to induce the translocation of BAX to mitochondria, the cyt-C release from these organelles (Figures 5S and 6S, SI), the activation of caspase 3, and the formation of apoptotic nuclei (Figures 5S and 7S, SI).

Similarly to what we have already shown in MEF $BAX^{-/-}$ cells, 8 treatment had no effects on the leukemic Jurkat (T-cell

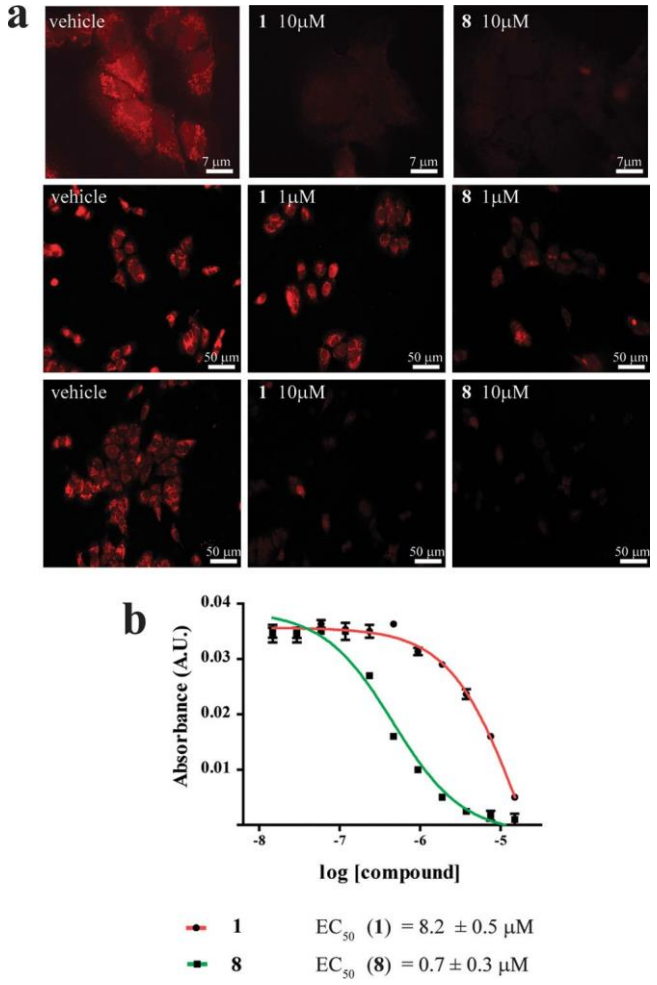

Figure 4. 8 affects mitochondria in HuH7 cells. (a) Mitochondrial activity of 8 and 1 treated cells visualized by Mitotracker Red fluorescence uptake. Magnification bars are indicated. (b) After lysis of the cells absorbance of the dye was measured at 570 nm and plotted versus 8 or 1 concentration. EC_{50} were calculated by fitting values by non linear regression analysis of dose response analysis and reported together with their 95% CI (error bars are indicated, $n = 3$).

lymphoma) cell line. Jurkat cells express a mutated form of BAX and rely only on BAK to induce MOMP.[18] Jurkat cells resulted insensitive to 8 treatment, confirming that our compound activates selectively BAX (Figure 6). Differently leukemic NB4 cells (promyelocytic), which express wt BAX,[19] showed hallmarks of apoptosis already after 12 h of treatment with 8.

Then, to have indication about the toxicity of 8 on healthy cells, we tested the effect of the compound on primary healthy splenocytes. At concentration of 10 μM, 8 did not alter the apoptosis rate in primary cells, indicating that could selectively affect tumoral cells (Figure 6). This observation could be explained by the fact that, as seen for many other cancer drugs, 8 could affect predominantly highly proliferating cells rather than resting ones.[20]

Compound 8 is able to affect mitochondrial membrane potential in all the tumor cell lines tested (Figure 5). Like HuH7, Lewis lung carcinoma (LLC1) and human neuroblastoma (SHSY-5Y) cells were reported to be highly resistant to conventional pro-apoptotic drugs. Like for HuH7, after treatment with 8, these cells did not show sign of death (visible

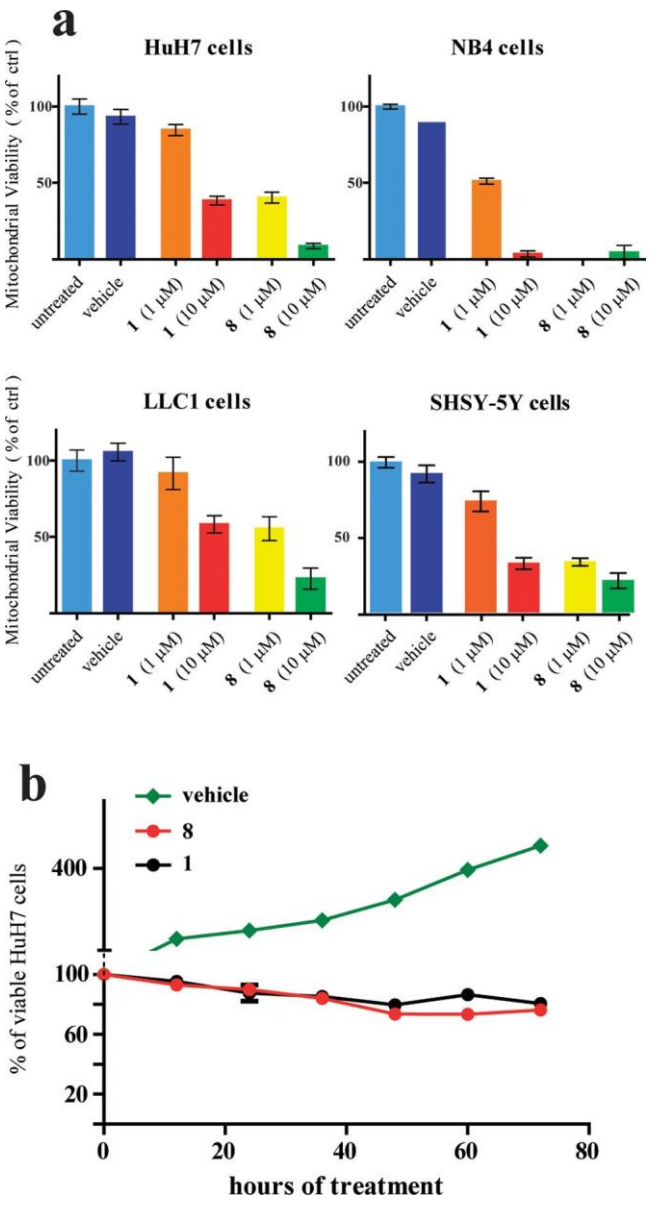

Figure 5. 8 induces growth arrest and cell death. (a) Cells were incubated for 72 h with the indicated concentration of 1 and 8 and then with Mitotracker. Absorbance was measured after lysis of the cell. Values are the mean of at least three experiment. Error bars (SD) are indicated. (b) HuH7 cells were incubated for the indicated time with 10 μ 1 or 8 or vehicle alone. After the treatment cells were counted. Values are expressed as percentage of control (cells at 0 min of treatment) and are representative of at least three experiments.

in only the 20% of cell (data not shown)), but they stop duplicating to undergo in a process of growth arrest. This effect likely suggests that even in those tumor cell lines that have developed strategies to block the initiation of the apoptotic process or its completion, BAX direct activation can hamper mitochondrial activity, reduce intracellular energy content, and ultimately affects cell growth.

In Situ BAX Activation and in Vivo Tests. LLC1 cells resulted sensitive to 8 (Figure 5). These cells well represent lung carcinoma, the primary cause of adult mortality. To establish whether 8 would be efficacious in vivo, we used them in a murine Lewis lung carcinoma model that reliably recapitulates human lung cancer in pathology, disease progression, clinical outcome, and response to therapies.[21] LLC1 cells have a high tropism for the lung and are able to form tumor lesions[22] that after 14 days are in exponential growth, making the drug treatment clinically relevant. On day 0, tumor cells were injected into mice via the tail vein. From day 14 to day 17, one group of mice were treated once a day with an intraperitoneal injection of 8 (1 mg/kg) or of vehicle (1% DMSO). On day 17, animals were euthanized. The compound ability to induce an in vivo activation of BAX was confirmed trough immunoprecipitation of lung lysates with 6A7 antibody (Figure 7). A visual inspection of the exposed lung of control mice showed very large tumor lesions covering the lung surface, whereas the lungs of mice treated with 8 showed highly size-reduced tumor lesions. Histological analysis using hematoxylin and eosin (H&E) staining of lung sections demonstrated that after only 4 days of treatment the ratio between tumor burden and lung area in mice treated with 8 compared with control was significantly ($P < 0.01$) decreased by 50% (Figure 8).

It is noteworthy that 8 seemed to be well tolerated because no mortalities, evidence of gross toxicity, behavioral side effects, or body weight changes were observed in the four days of treatments.

A microscopic examination of heart, femoral muscle, and healthy lung did not reveal any pathologic change (data not shown). The in vivo efficiency of 8 in tumor mass reduction was of relevance especially if a rough comparison with marketed anticancer drugs on similar tumor models is done. In fact, cyclophosphamide (60 mg/kg) or adriamycin (1.25 mg/kg) gave a reduction of 40% even in the case of prolonged treatments.[23,24]

CONCLUSION

Optimization of BAX direct activators has been already shown to be challenging.[11] We here show that 1 optimization can successfully lead to new hits with improved affinity for BAX. However, minimal changes in the chemical structure of the hits can drastically change their selectivity, affecting their affinity for other BCL-2 family members. In MEF cells, whatever the main target is, the event of binding leads always to apoptosis. However, in tumor cells, a severe unbalancing between pro-apopototic and antiapopototic proteins exists, with the latter being overexpressed in almost every tumor. Thus, ligands with low selectivity can be sequestered by antiapoptotic proteins that, ultimately, buffer them, inhibiting the activation of pro-apoptotic proteins.

As a result of our first round of 1 optimization, we here present 8. In vitro affinity of 8 for BAX is only slightly higher than 1. On the contrary, it shows lower affinity for BCL-2 and BCL-X_L than 1. Its selectivity manifests in MEF BAX$^{-/-}$ knockout cells that, differently from many other tested MEF knockout clones, are insensitive to 8 treatments. In cultured tumor cells, it induces MOMP with an EC_{50} of 700 nM, 1 order of magnitude lower than the one measured for 1. As such, it is the most active, low molecular weight, direct activator of BAX reported in the published literature. SAR data here developed clearly suggest that the phenyl-thiazol moiety can be replaceable by other aromatic groups and that the activity is increased by a terminal positive charged group that, according to a theoretical binding mode, would interact with negatively charged BAX residues. 8 is able to induce BAX activation and translocation to mitochondria, MOMP, and consequent release of cyt-C in all the tumor cell line tested. Moreover, 8 seems to be rather selective for cancer cells (HuH7, NB4, SHSY-5Y, and

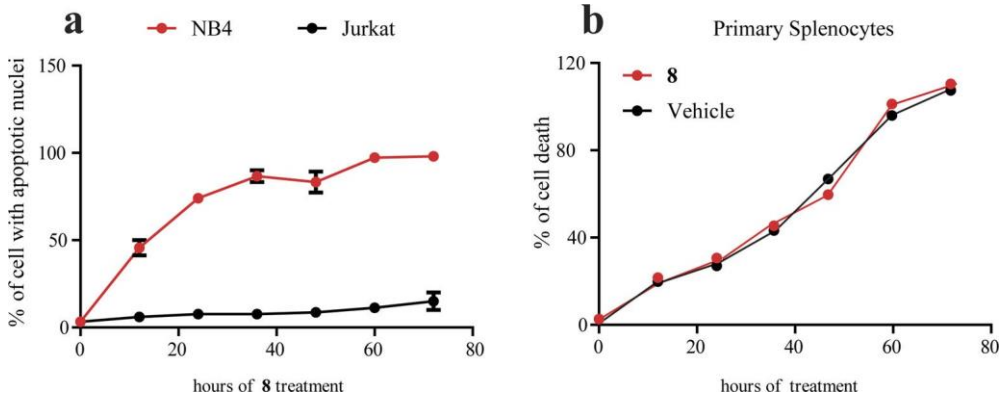

Figure 6. 8 induces apoptosis in tumor cells but it does not alter apoptotic rate in healthy splenocytes. The indicated tumor cell lines (a) or primary splenocytes (b) were incubated for 72 h with 8 (10 μM). Apoptosis rates were detected by counting apopototic nuclei. Mean values are reported together with their SD (n = 3 in a; n = 4 in b).

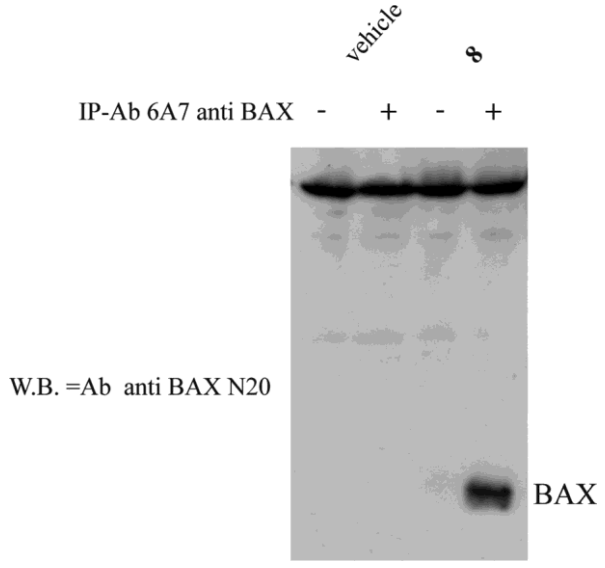

Figure 7. In vivo treatment with 8 induces in situ BAX activation. Homogenates of mouse lungs treated or not with 8 were lysed and immunoprecipitated with the 6A7 monoclonal antibody. Samples were boiled, run on a SDS-PAGE, and decorated with a polyclonal antibody anti-BAX (only relevant part of the gel is shown).

LLC1) and immortalized cells (MEF), leaving unperturbed apoptosis rate in healthy resting cells (healthy splenocytes).

The in vivo efficiency of 8 in tumor mass reduction together with the absence of gross toxicity, although just 4 days of treatment was applied, would suggest that BAX direct activators may really represent a novel promising class of anticancer agents rather than venoms.

EXPERIMENTAL SECTION

Chemistry. All reagents and solvents were handled according to material safety data sheet of the supplier and were used as purchased without further purification. Organic solutions were dried over anhydrous sodium sulfate. Evaporation of the solvents was carried out on Büchi Rotavapor R-210 equipped with Büchi V-855 vacuum controller and Büchi V-700 (~5 mbar) and V-710 (~2 mbar) vacuum pumps and on Heidolph Hei-Vap G3B equipped with Vacuubrand PC 3001 vacuum pump (~2 mbar). Column chromatography was performed on glass columns packed with silica gel from Fluka and from Aldrich (70−230 mesh). Silica gel thin layer chromatography (TLC) cards from Fluka and Macherey-Nagel (silica gel precoated aluminum cards with fluorescent indicator visualizable at 254 nm)

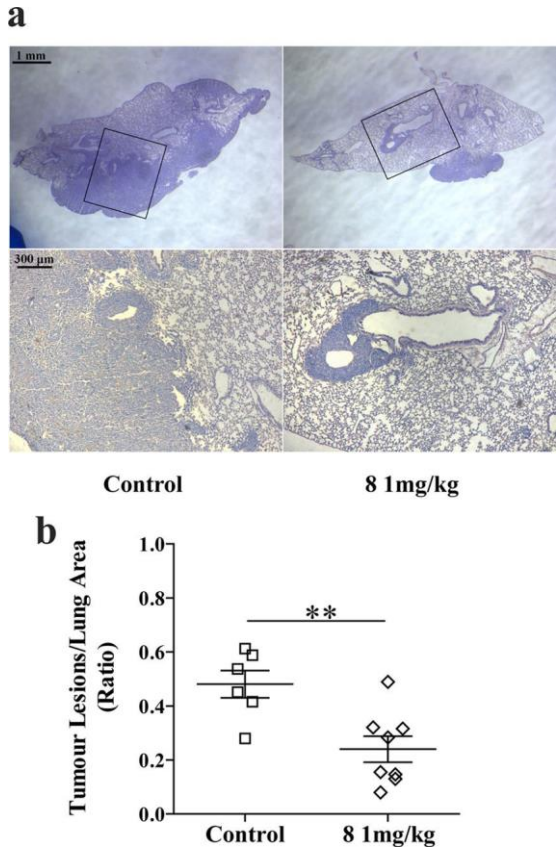

Figure 8. In vivo activity of 8. (a) Effect of the daily administration of 8 1 mg/kg from day 14 to day 17 on tumor growth (dark violet staining). Microphotographs showing the entire lung sections; the boxed areas in the upper-magnification H&E panels are shown at a higher magnification in the lower panels. (b) Graph showing the effect of 8 on tumor growth. The results are expressed as tumor lesions/lung area ratio. Individual data points represent average value per mouse; horizontal bars denote mean. $P < 0.01$ vs control group.

were used for TLC. Developed plates were visualized by a Spectroline ENF 260C/FE UV apparatus. Melting points (mp) were determined on a Stuart Scientific SMP1 apparatus and on a Stuart Scientific SMP30 apparatus and are uncorrected. Infrared spectra (IR) were run on PerkinElmer SpectrumOne FT-ATR spectrophotometer. Band position and absorption ranges are given in cm^{-1}. Mass spectral (MS) and high resolution mass spectral (HRMS) analyses were recorded on AB Sciex API-2000 (MS) and Thermo Fisher Scientific Inc. Orbitrap

Exactive (HRMS) spectrometers equipped with an ESI source. Proton (^{1}H, 400.13 MHz) and carbon (^{13}C, 100.6 MHz) nuclear magnetic resonance spectra were recorded on a Bruker Avance 400 and a Varian Inova 400 spectrometers in the indicated solvent and corresponding fid files processed by MestreLab Research SL MestreReNova 6.2.1−769 and Bruker Topspin 3.2 software. Chemical shifts are expressed in δ units (ppm) from tetramethylsilane. Elemental analyses of the compounds were found within ±0.4% of the theoretical values. The purity of tested compounds was found to be >95% by high pressure liquid chromatography (HPLC) analysis. The HPLC system used (Thermo Fisher Scientific Inc. Dionex UltiMate 3000) consisted of a SR-3000 solvent rack, a LPG-3400SD quaternary analytical pump, a TCC-3000SD column compartment, a DAD-3000 diode array detector, and an analytical manual injection valve with a 20 μL loop. Samples were dissolved in acetonitrile at 10 mg/mL. HPLC analysis was performed by using a Thermo Fisher Scientific Inc. Acclaim 120 C18 reversed-phase column (5 μm, 4.6 mm × 250 mm) at 30 ± 1 °C with an isocratic gradient (acetonitrile:water = 90:10), flow rate of 1.0 mL/min, and signal detector at 254 and 365 nm. Chromatographic data were acquired and processed by Thermo Fisher Scientific Inc. Chromeleon 6.80 software.

General Procedure for the Preparation of Compounds 2−5 and 16. *Example: 4-(2,2-Diphenylethylidene)-3-methyl-1-(4-phenylthiazol-2-yl)-1H-1H-pyrazol-5(4H)-one (2).* A mixture of 17 (0.21 g, 0.00084 mol), 2,2-diphenylacetaldehyde (0.16 g, 0.15 mL, 0.84 mmol), and piperidine (0.071 g, 0.08 mL, 0.84 mmol) in ethanol (0.5 M) were heated to reflux for 3 h and evaporated. The residue was purified by column chromatography (silica gel, dichloromethane:methanol = 99:1 as eluent) to furnish 2 (0.17 g, 47%), mp >220 °C with decomposition (from ethanol). ^{1}H NMR (DMSO-d_6): δ 1.53 (s, 3H), 6.49 (s, 1H), 7.16 (d, J = 3.7 Hz, 2H), 7.22−7.38 (m, 10H), 7.43 (t, J = 7.4 Hz, 2H), 7.72 (s, 1H), 7.96 ppm (d, J = 3.8 Hz, 2H). IR: ν 1616 cm^{-1}. Anal. ($C_{27}H_{21}N_3OS$ (435.54)): C, 74.46; H, 4.86; N, 9.65; S, 7.36. Found: C, 74.44; H, 4.83; N, 9.69; S, 7.34. MS (ESI) calcd for $C_{27}H_{21}N_3OS$: 435.1; found (M + H)$^+$: 436.1.

4-([1,1′-Biphenyl]-4-ylmethylene)-3-methyl-1-(4-phenylthiazol-2-yl)-1H-pyrazol-5(4H)-one (3). It was synthesized as 2 starting from 17 and [1,1′-biphenyl]-4-carbaldehyde. Yield 61%, mp >270 °C with decomposition (from ethanol). ^{1}H NMR (DMSO-d_6): δ 2.13 (s, 3H), 7.29−7.38 (m, 4H), 7.40−7.48 (m, 5H), 7.58−7.68 (m, 4H), 7.72 (s, 1H), 7.98 (d, J = 3.7 Hz, 2H). IR: ν 1625 cm^{-1}. Anal. ($C_{26}H_{19}N_3OS$ (421.51)): C, 74.08; H, 4.54; N, 9.97; S, 7.61. Found: C, 74.04; H, 4.58; N, 9.92; S, 7.59. MS (ESI) calcd for $C_{26}H_{19}N_3OS$: 421.1; found (M + H)$^+$: 422.3.

3-Methyl-4-(naphthalen-2-ylmethylene)-1-(4-phenylthiazol-2-yl)-1H-pyrazol-5(4H)-one (4). It was synthesized as 2 starting from 17 and 2-naphthaldehyde. Yield 37%, mp >270 °C with decomposition (from ethanol). ^{1}H NMR (DMSO-d_6): δ 2.07 (s, 3H), 7.29−7.38 (m, 1H), 7.39−7.50 (m, 5H), 7.70 (s, 1H), 7.75 (s, 1H), 7.80−7.90 (m, 3H), 7.93−8.03 ppm (m, 3H). IR: ν 1615 cm^{-1}. Anal. ($C_{24}H_{17}N_3OS$ (395.48)): C, 72.89; H, 4.33; N, 10.63; S, 8.11. Found: C, 72.86; H, 4.31; N, 10.59; S, 8.09. MS (ESI) calcd for $C_{24}H_{17}N_3OS$:, 395.1; found (M + H)$^+$: 396.1.

4-((1H-Imidazol-2-yl)methylene)-3-methyl-1(4-phenylthiazol-2-yl)-1H-pyrazol-5(4H)-one (5). It was synthesized as 2 starting from 17 and 1*H*-imidazole-2-carbaldehyde. Yield 28%, mp 189−191 °C (from ethanol). ^{1}H NMR (DMSO-d_6): δ 1.98 (s, 3H), 7.18 (s, 1H), 7.26−7.48 (m, 5H), 7.62 (d, J = 3.6 Hz, 1H), 7.69 (s, 1H), 7.92 ppm (d, J = 3.8 Hz, 2H). IR: ν 1615 cm^{-1}. Anal. ($C_{17}H_{13}N_5OS$ (335.38)): C, 60.88; H, 3.91; N, 20.88; S, 9.56. Found: C, 60.87; H, 3.90; N, 20.86; S, 9.54. MS (ESI) calcd for $C_{17}H_{13}N_5OS$: 335.1; found (M + H)$^+$: 336.2.

4-Benzylidene-3-methyl-1-(4-phenylthiazol-2-yl)-1H-pyrazol-5(4H)-one (16). It was synthesized as 2 starting from 17 and benzaldehyde. Yield 30%, mp >270 °C with decomposition (from ethanol). ^{1}H NMR (DMSO-d_6): δ 2.07 (s, 3H), 7.17−7.23 (m, 1H), 7.24−7.35 (m, 5H), 7.39−7.46 (m, 3H), 7.70 (s, 1H), 7.97 ppm (d, J = 3.7 Hz, 2H). IR: ν 1360, 1495, 1622 cm^{-1}. Anal. ($C_{20}H_{15}N_3OS$ (345.42)): C, 69.54; H, 4.38; N, 12.17; S, 9.28. Found: C, 69.50; H, 4.36; N, 12.17; S, 9.26. MS (ESI) calcd for $C_{20}H_{15}N_3OS$: 345.1; found (M + H)$^+$: 346.2.

4-(2-(2-Ethoxyphenyl)acetyl)-3-methyl-1-(4-phenylthiazol-2-yl)-1H-pyrazol-5(4H)-one (6). A suspension of potassium *tert*-butoxide (0.13 g, 1.2 mmol) in anhydrous tetrahydrofuran (15.0 mL) was cooled at −40 °C, and a solution of 17 (0.25 g, 0.97 mmol) in the same solvent (10.0 mL) was added dropwise under Ar stream. The reaction mixture was stirred in the same conditions for 1 h, and a solution of 2-(2-ethoxyphenyl)acetyl chloride (0.31 g, 1.2 mmol) in the same solvent (5.0 mL) was added dropwise. The reaction mixture was stirred at 25 °C for 1 h, diluted with water, and extracted with ethyl acetate. Organic layer was washed with brine, dried, and filtered. Evaporation of the solvent gave a residue that was purified by column chromatography (silica gel, ethyl acetate:*n*-hexane = 1:1 as eluent) to furnish 6 (0.3 g, 74%), mp 105−110 °C (from ethanol). ^{1}H NMR (DMSO-d_6): δ 1.22 (t, J = 6.9 Hz, 3H), 2.25 (s, 3H), 3.97−4.02 (m, 4H), 6.26 (s, 1H), 6.85 (t, J = 7.3 Hz, 1H), 6.99 (d, J = 8.2 Hz, 1H), 7.16 (d, J = 6.4 Hz, 1H), 7.24 (t, J = 8.0 Hz, 1H), 7.40 (t, J = 7.2 Hz, 1H), 7.50 (t, J = 7.8 Hz, 2H), 7.90−7.94 ppm (m, 3H). IR: ν 1780, 1784 cm^{-1}. Anal. ($C_{23}H_{21}N_3O_3S$ (419.50)): C, 65.85; H, 5.05; N, 10.02; S, 7.64. Found: C, 65.80; H, 5.02; N, 10.06; S, 7.60. MS (ESI) calcd for $C_{23}H_{21}N_3O_3S$: 419.1; found (M + H)$^+$: 420.0. 2-(2-Ethoxyphenyl)acetyl chloride: A mixture of 2-(2-hydroxyphenyl)acetic acid (2.0 g, 13 mmol) and 37% hydrochloric acid (1.2 mL) in 96 ° ethanol (70.0 mL) was heated to reflux for 3 h, cooled, diluted with water, and extracted with ethyl acetate. The organic layer was washed with brine, dried, and filtered. Removal of the solvent gave ethyl 2-(2-hydroxyphenyl)acetate (2.22 g, 94%), mp 65−67 °C (from petroleum ether), lit. 67−68 °C.[25] A mixture of ethyl 2-(2-hydroxyphenyl)acetate (2.22 g, 12 mmol), anhydrous potassium carbonate (3.69 g, 26 mmol), and iodoethane (4.11 g, 2.1 mL, 26 mmol) in anhydrous *N*,*N*-dimethylformamide (10.0 mL) was heated at 50 °C for 12 h. After cooling, the reaction mixture was diluted with water and extracted with ethyl acetate. The organic layer was washed with brine, dried, and filtered. Removal of the solvent gave a residue that was purified by column chromatography (silica gel, ethyl acetate:*n*-hexane = 3:7 as eluent) to furnish ethyl 2-(2-ethoxyphenyl)acetate (2.22 g, 86%), oil. ^{1}H NMR (DMSO-d_6): δ 1.16 (t, J = 7.1 Hz, 3H), 1.27 (t, J = 6.9 Hz, 3H), 3.55 (s, 2H), 3.96−4.07 (m, 4H), 6.86 (t, J = 7.4 Hz, 1H), 6.93 (d, J = 8.1 Hz, 1H), 7.15−7.23 ppm (m, 2H). IR: ν 1733 cm^{-1}. A mixture of ethyl 2-(2-ethoxyphenyl)acetate (4.86 g, 23 mmol) in 3N sodium hydroxide/96° ethanol (1:1, v/v) (180.0 mL) was heated to reflux for 12 h. After cooling, the reaction mixture was made acidic with 6N hydrogen chloride and extracted with ethyl acetate. The organic layer was washed with brine, dried, and filtered. Removal of the solvent gave 2-(2-ethoxyphenyl)acetic acid (3.50 g, 83%), mp 99−102 °C (from ethanol), lit 103 °C.[26] ^{1}H NMR (DMSO-d_6): δ 1.28 (t, J = 6.7 Hz, 3H), 3.48 (s, 2H), 3.98 (q, J = 6.8 Hz, 2H), 6.85 (t, J = 6.9 Hz, 1H), 6.93 (d, J = 8.0 Hz, 1H), 7.14−7.31 (m, 2H), 12.13 ppm (broad s, disappeared on treatment with D_2O, 1H). IR: ν 1730, 2987 cm^{-1}. To a mixture of 2-(2-ethoxyphenyl)acetic acid (0.21 g, 1.2 mol) in anhydrous benzene (9.0 mL) was added thionyl chloride (1.45 g, 0.9 mL, 12 mmol). The reaction mixture was stirred at 25 °C for 1 h and evaporated to give 2-(2-ethoxyphenyl)acetyl chloride that was used without further purification.

1-(2-Ethoxyphenyl)-2-(3-methyl-5-oxo-1-(4-phenylthiazol-2-yl)-4,5-dihydro-1H-pyrazol-4-yl)ethane-1,2-dione (7). A mixture of 6 (0.25 g, 0.59 mmol), potassium permanganate (0.38 g, 2.4 mmol), and a catalytic amount of 98% sulfuric acid in acetone (10.0 mL) was heated to reflux for 12 h. Removal of the solvent gave a residue that was purified by column chromatography (silica gel, ethyl acetate:*n*-hexane = 3:7 as eluent) to furnish 7 (0.013 g, 5%), mp 108−110 °C (from ethanol). ^{1}H NMR (DMSO-d_6): δ 1.22 (t, J = 6.8 Hz, 3H), 2.29 (s, 3H), 4.06 (d, J = 6.7 Hz, 2H), 6.39 (s, 1H), 7.12−7.28 (m, 5H), 7.53 (d, J = 7.4 Hz, 2H), 7.74 (m, 1H), 7.86 (s, 1H), 8.19 ppm (d, J = 6.6 Hz, 1H). IR: ν 1215, 2926 cm^{-1}. Anal. ($C_{23}H_{19}N_3O_4S$ (433.48)): C, 63.73; H, 4.42; N, 9.69; S, 7.40. Found: C, 63.70; H, 4.39; N, 9.72; S, 7.38. MS (ESI) calcd for $C_{23}H_{19}N_3O_4S$: 433.1; found (M + H)$^+$: 434.4.

General Procedure for the Preparation of Compounds 8, 12, 15, and 22–26. *Example: 1-(4′-(Dimethylamino)-5-hydroxy-[1,1′-biphenyl]-3-yl)-4-(2-(2-ethoxyphenyl)hydrazono)-3-methyl-1H-pyrazol-5(4H)-one (8).* A mixture of 20 (0.07 g, 0.17 mmol), 2 M sodium carbonate (0.3 mL), and (4-(dimethylamino)phenyl)boronic acid (0.034 g, 0.21 mmol) in tetrahydrofuran (0.6 mL) was degassed for 10 min. Dichloro[1,1′-bis(diphenylphosphino)ferrocene]-palladium(II) (0.0082 g, 0.01 mmol; complex with dichloromethane (1:1), Pd 13%) was added, and the reaction mixture was stirred at reflux temperature for 90 min under Ar stream, cooled, diluted with water, and extracted with ethyl acetate. Organic layer was washed with brine, dried, and filtered. Removal of the solvent gave a residue that was purified by column chromatography (silica gel, ethyl acetate:*n*-hexane = 7:3 as eluent) to furnish 8 (0.010 g, 13%), mp 230–232 °C (from ethanol). ^{1}H NMR (DMSO-d_6): δ 1.42 (t, J = 7.1 Hz, 3H), 2.32–2.49 (m, 6H), 2.94 (s, 3H), 4.23 (q, J = 7.1 Hz, 2H), 6.78–6.80 (m, 2H), 7.08 (s, 1H), 7.20 (s, 2H), 7.35 (s, 1H), 7.44–7.46 (d, J = 7.8 Hz, 2H), 7.53–7.70 (m, 3H), 9.71 (broad s, disappeared on treatment with D_2O, 1H), 13.60 ppm (broad s, disappeared on treatment with D_2O, 1H). ^{13}C NMR (DMSO-d_6): δ 11.97, 15.08, 40.47, 65.12, 103.47, 106.73, 109.75, 113.05, 113.72, 114.72, 122.08, 126.70, 127.49, 128.04, 129.12, 130.59, 139.66, 142.67, 147.58, 148.34, 157.71, 158.55. IR: ν 1656, 2854, 2924 cm^{-1}. Anal. ($C_{26}H_{27}N_5O_3$ (457.52)): C, 68.25; H, 5.95; N, 15.31. Found: C, 68.22; H, 5.90; N, 15.29. HRMS (ESI) calcd for $C_{26}H_{27}N_5O_3$: 457.2114; found $(M - H)^-$: 456.2021.

2-(3′-Amino-5-hydroxy-[1,1′-biphenyl]-3-yl)-4-(2-(2-ethoxyphenyl)hydrazono)-5-methyl-2,4-dihydro-3H-pyrazol-3-one (12). It was synthesized as 8 starting from 20 and (3-aminophenyl)-boronic acid. Yield 66%, mp 180–183 °C (from ethanol). ^{1}H NMR (DMSO-d_6): δ 1.42 (t, J = 7.2 Hz, 3H), 2.31 (s, 3H), 4.21 (q, J = 7.1 Hz, 2H), 5.19 (broad s, disappeared on treatment with D_2O, 2H), 6.56 (d, J = 6.9 Hz, 1H), 6.70 (d, J = 7.3 Hz, 1H), 6.76–6.80 (m, 2H), 7.03–7.11 (m, 2H), 7.19 (s, 2H), 7.44 (s, 1H), 7.52 (s, 1H), 7.71 (d, J = 8.3 Hz, 1H), 9.75 (broad s, disappeared on treatment with D_2O, 1H), 13.59 ppm (broad s, disappeared on treatment with D_2O, 1H). IR: ν 1693, 2852, 2922, 3271 cm^{-1}. Anal. ($C_{24}H_{23}N_5O_3$ (429.48)): C, 67.12; H, 5.40; N, 16.31. Found: C, 67.10; H, 5.38; N, 16.29. MS (ESI) calcd for $C_{23}H_{19}N_3O_4S$: 429.2; found $(M + H)^+$: 430.1.

2-(4′-(Dimethylamino)-5-hydroxy-[1,1′-biphenyl]-3-yl)-5-methyl-4-(2-(naphthalen-2-yl)hydrazono)-2,4-dihydro-3H-pyrazol-3-one (15). It was synthesized as 8 starting from 21 and (4-(dimethylamino)-phenyl)boronic acid. Yield 18%, mp 221–226 °C (from ethanol). ^{1}H NMR (DMSO-d_6): δ 2.35 (s, 3H), 2.93 (s, 6H), 3.76–6.81 (m, 3H), 7.29 (s, 1H), 7.38–7.49 (m, 3H), 7.54–7.56 (m, 1H), 7.70 (s, 1H), 7.85–7.93 (m, 3H), 8.00–8.07 (m, 2H), 9.67 (broad s, disappeared on treatment with D_2O, 1H), 13.59 ppm (broad s, disappeared on treatment with D_2O, 1H). IR: ν 1655, 1736, 2852, 2922, cm^{-1}. Anal. ($C_{28}H_{25}N_5O_2$ (463.20)): C, 72.55; H, 5.44; N, 15.11. Found: C, 72.53; H, 5.46; N, 15.10. MS (ESI) calcd for $C_{28}H_{25}N_5O_2$: 463.2; found $(M + H)^+$: 463.3.

1-(5-Hydroxy-[1,1′-biphenyl]-3-yl)-3-methyl-1H-pyrazol-5(4H)-one (22). It was synthesized as 8 starting from 19 and phenylboronic acid. Yield 60%, mp 160–163 °C (from ethanol). ^{1}H NMR (DMSO-d_6): δ 2.36 (s, 3H), 6.88 (s, 1H), 7.35–7.37 (m, 2H), 7.43–7.46 (m, 3H), 7.60–7.62 (m, 3H), 9.84 (broad s, disappeared on treatment with D_2O, 1H), 12.12 ppm (broad s, disappeared on treatment with D_2O, 1H). IR: ν 1599, 1685, 3063 cm^{-1}.

1-(3-Hydroxy-5-(thiophen-2-yl)phenyl)-3-methyl-1H-pyrazol-5(4H)-one (23). It was synthesized as 8 starting from 19 and thiophen-2-ylboronic acid. Yield 32%, mp 175–178 °C (from ethanol). ^{1}H NMR (DMSO-d_6): δ 2.10 (s, 3H), 5.37 (s, 1H), 6.87 (s, 1H), 7.12–7.16 (m, 2H), 7.41–7.45 (m, 2H), 7.53 (s, 1H), 9.78 (broad s, disappeared on treatment with D_2O, 1H), 11.56 ppm (broad s, disappeared on treatment with D_2O, 1H). IR: ν 1587, 1679, 3091 cm^{-1}.

2-(5-Hydroxy-4′-isopropyl-[1,1′-biphenyl]-3-yl)-5-methyl-2,4-dihydro-3H-pyrazol-3-one (24). It was synthesized as 8 starting from 19 and (4-isopropylphenyl)boronic acid and was used without further purification.

3-Nitro-5-(pyridin-4-yl)phenol (25). It was synthesized as 8 starting from 3-bromo-5-nitrophenol[27] and pyridin-4-ylboronic acid. Yield 14%, mp 200 °C with decomposition (from ethanol). ^{1}H NMR (DMSO-d_6): δ 7.56–7.61 (m, 1H), 7.63–7.64 (m, 1H), 7.74–7.75 (m, 2H), 7.98–8.00 (m, 1H), 8.64–8.67 ppm (m, 2H), 10.76 ppm (broad s, disappeared on treatment with D_2O, 1H). IR: ν 2923 cm^{-1}.

4′-(Dimethylamino)-5-nitro-[1,1′-biphenyl]-3-ol (26). It was synthesized as 8 starting from 1-bromo-3-nitrobenzene and (4-(dimethylamino)phenyl)boronic acid. Yield 25%, mp 130–134 °C (from ethanol). ^{1}H NMR (DMSO-d_6): δ 2.95 8s, 6H), 6.80–6.84 (m, 2H), 7.61–7.68 (m, 3H), 8.04–8.07 (m, 2H), 8.33 ppm (m, 1H).

General Procedure for the Preparation of Compounds 9–11, 13, 14, 20, and 21. *Example: 4-(2-(2-Ethoxyphenyl)-hydrazono)-1-(5-hydroxy-[1,1′-biphenyl]-3-yl)-3-methyl-1H-pyrazol-5(4H)-one (9).* A mixture of 22 (0.054 g, 0.000203 mol) and sodium acetate (0.028 g, 0.20 mmol) in 96° ethanol (1.1 mL) was cooled at 0 °C. 2-Ethoxybenzenediazonium chloride (0.02 mmol) was added, and the reaction mixture was stirred at the same temperature for 2 h, diluted with water, and extracted with ethyl acetate. The organic layer was washed with brine, dried, and filtered. Removal of the solvent gave a residue that was purified by column chromatography (silica gel, ethyl acetate:*n*-hexane = 7:3 as eluent) to furnish 9 (0.070 g, 8%), mp 163–166 °C (from ethanol). ^{1}H NMR (DMSO-d_6): δ 1.42 (t, J = 6.9 Hz, 3H), 2.32 (s, 3H), 4.22 (q, J = 7.0 Hz, 2H), 6.86 (s, 1H), 7.06–7.08 (m, 1H), 7.19–7.21 (m, 2H), 7.36–7.38 (m, 1H), 7.47–7.49 (m, 3H), 7.58–7.60 (m, 3H), 7.69–7.71 ppm (m, 1H), 9.84 (broad s, disappeared on treatment with D_2O, 1H), 13.59 ppm (broad s, disappeared on treatment with D_2O, 1H). IR: ν 1594, 1663, 2924, 3149 cm^{-1}. Anal. ($C_{24}H_{22}N_4O_3$ (414.46)): C, 69.55; H, 5.35; N, 13.52. Found: C, 69.53; H, 5.30; N, 13.54. MS (ESI) calcd for $C_{24}H_{22}N_4O_3$: 414.2; found $(M + H)^+$: 415.1. 2-Ethoxybenzenediazonium chloride: 1-Ethoxy-2-nitrobenzene was synthesized as ethyl 2-(2-ethoxyphenyl)acetate[28] starting from 2-nitrophenol and iodoethane. Yield 90%, yellow oil. A solution of 1-ethoxy-2-nitrobenzene (0.10 g, 0.6 mmol) in methanol (15.0 mL) was treated with hydrogen gas (30 psi) in the presence of palladium on carbon (0.01 g) at 25 °C for 2 h, filtered, and evaporated to give 2-ethoxyaniline that was used without further purification. To a cold solution of crude 2-ethoxyaniline (0.05 g, 0.36 mmol) in 37% hydrogen chloride (0.7 mL), a solution of sodium nitrite (0.025 g, 0.36 mmol) in water (0.2 mL) was added dropwise. The reaction mixture was stirred at 0 °C for 20 min to give 2-ethoxybenzenediazonium chloride that was used without further purification.

4-(2-(2-Ethoxyphenyl)hydrazono)-1-(3-hydroxy-5-(pyridin-4-yl)-phenyl)-3-methyl-1H-pyrazol-5(4H)-one (10). It was synthesized as 9 starting from 29 and 2-ethoxybenzenediazonium chloride. Yield 36%, slurry. ^{1}H NMR (DMSO-d_6): δ 1.43 (t, J = 7.0 Hz, 3H), 2.33 (s, 3H), 4.24 (q, J = 7.0 Hz, 2H), 7.10–7.12 (m, 2H), 7.20–7.22 (m, 2H), 7.78 (m, 3H), 8.00–8.10 (m, 2H), 8.84–8.86 (m, 2H), 10.22 7.71 (broad s, disappeared on treatment with D_2O, 1H), 13.55 ppm (broad s, disappeared on treatment with D_2O, 1H). IR: ν 1732, 2583, 2855, 2896 cm^{-1}. Anal. ($C_{23}H_{21}N_5O_3$ (415.44)): C, 66.49; H, 5.09; N, 16.86. Found: C, 66.47; H, 5.11; N, 16.84. MS (ESI) calcd for $C_{23}H_{21}N_5O_3$: 415.2; found $(M + H)^+$: 415.9.

4-(2-(2-Ethoxyphenyl)hydrazono)-1-(3-hydroxy-5-(thiophen-2-yl)phenyl)-3-methyl-1H-pyrazol-5(4H)-one (11). It was synthesized as 9 starting from 23 and 2-ethoxybenzenediazonium chloride. Yield 3%, mp 165–167 °C (from ethanol). ^{1}H NMR (DMSO-d_6): δ 1.42 (t, J = 7.0 Hz, 3H), 2.32 (s, 3H), 4.22 (q, J = 7.1 Hz, 2H), 6.90 (s, 1H), 7.08–7.09 (m, 1H), 7.14–7.15 (m, 1H), 7.20–7.22 (m, 2H), 7.42–7.44 (m, 2H), 7.55–7.56 (m, 1H), 7.61–7.63 (m, 1H), 7.69–7.71 (m, 1H), 9.89 (broad s, disappeared on treatment with D_2O, 1H), 13.59 ppm (broad s, disappeared on treatment with D_2O, 1H). IR: ν 1661, 1730, 2854, 2923, 2956 cm^{-1}. Anal. ($C_{22}H_{20}N_4O_3S$ (420.48)): C, 62.84; H, 4.79; N, 13.32; S, 7.63. Found: C, 62.82; H, 4.78; N, 13.29; S, 7.61. MS (ESI) calcd for $C_{22}H_{20}N_4O_3S$: 420.1; found $(M + H)^+$: 421.0.

4-(2-(2-Ethoxyphenyl)hydrazono)-1-(5-hydroxy-4′-isopropyl-[1,1′-biphenyl]-3-yl)-3-methyl-1H-pyrazol-5(4H)-one (13). It was synthesized as 9 starting from 24 and 2-ethoxybenzenediazonium chloride. Yield 17%, slurry. ^{1}H NMR (DMSO-d_6): δ 1.22 (s, 3H), 1.24 (s, 3H), 1.42 (t, J = 7.0 Hz, 3H), 1.98 (s, 3H), 2.91–2.94 (m, 1H),

4.02 (q, J = 6.2 Hz, 2H), 6.84−6.86 (m, 1H), 7.08−7.10 (m, 1H), 7.19−7.21 (m, 2H), 7.33−7.35 (m, 2H), 7.44−7.46 (m, 1H), 7.50−7.53 (m, 2H), 7.58−7.60 (m, 1H), 7.70−7.72 (m, 1H), 9.79 (broad s, disappeared on treatment with D_2O, 1H), 13.59 ppm (broad s, disappeared on treatment with D_2O, 1H). IR: ν 1655, 1728, 2854, 2924, 2958 cm^{-1}. Anal. ($C_{27}H_{28}N_4O_3$ (456.54)): C, 71.03; H, 6.18; N, 12.27. Found: C, 71.00; H, 6.16; N, 12.29. MS (ESI) calcd for $C_{27}H_{28}N_4O_3$: 456.2; found $(M + H)^+$: 456.3.

1-(4′-(Dimethylamino)-[1,1′-biphenyl]-3-yl)-4-(2-(2-ethoxyphenyl)hydrazono)-3-methyl-1H-pyrazol-5(4H)-one (14). It was synthesized as 9 starting from 30 and 2-ethoxybenzenediazonium chloride. Yield 47%, 230−232 °C (from ethanol). ^1H NMR (DMF-d_7): δ 1.67 (t, J = 7.0 Hz, 3H), 2.56 (s, 3H), 3.18 (s, 6H), 4.47 (q, J = 6.9 Hz, 2H), 7.06 (d, J = 8.8 Hz, 2H), 7.28−7.30 (m, 1H), 7.40−7.43 (m, 2H), 7.67−7.69 (m, 2H), 7.76−7.78 (d, J = 8.9 Hz, 2H), 7.96 (d, J = 7.5 Hz, 1H), 8.01−8.13 (m, 1H), 8.41 (s, 1H), 13.98 ppm (broad s, disappeared on treatment with D_2O, 1H). IR: ν 1652, 1713, 2851, 2922 cm^{-1}. Anal. ($C_{26}H_{27}N_5O_2$ (441.52)): C, 70.73; H, 6.16; N, 15.86. Found: C, 70.71; H, 6.14; N, 15.84. MS (ESI) calcd for $C_{26}H_{27}N_5O_2$: 441.2; found $(M + H)^+$: 441.3.

1-(3-Bromo-5-hydroxyphenyl)-4-(2-(2-ethoxyphenyl)hydrazono)-3-methyl-1H-pyrazol-5(4H)-one (20). It was synthesized as 9 starting from 19 and 2-ethoxybenzenediazonium chloride. Yield 48%, mp 215−217 °C (from ethanol). ^1H NMR (DMSO-d_6): δ 1.43 (t, J = 7.0 Hz, 3H), 2.29 (s, 3H), 4.22 (q, J = 6.9 Hz, 2H), 6.78 (s, 1H), 7.06−7.09 (m, 1H), 7.19−7.21 (m, 2H), 7.45 (s, 1H), 7.55 (s, 1H), 7.69−7.70 (m, 1H), 10.15 (broad s, disappeared on treatment with D_2O, 1H), 13.50 ppm (broad s, disappeared on treatment with D_2O, 1H). IR: ν 1661, 2934, 2979, 3121 cm^{-1}.

1-(3-Bromo-5-hydroxyphenyl)-3-methyl-4-(2-(naphthalen-2-yl)-hydrazono)-1H-pyrazol-5(4H)-one (21). It was synthesized as 9 starting from 19 and naphthalene-2-diazonium chloride. Yield 7%, mp 233−237 °C (from ethanol). ^1H NMR (DMSO-d_6): δ 1.22 (s, 3H), 6.78 (s, 1H), 7.43−7.47 (m, 2H), 7.52−7.55 (m, 1H), 7.64−7.66 (m, 2H), 7.5−7.87 (m, 1H), 7.90−7.92 (m, 2H), 8.01−8.20 (m, 1H), 8.07 (broad s, disappeared on treatment with D_2O, 1H), 10.16 ppm (broad s, disappeared on treatment with D_2O, 1H). IR: ν 1731, 2853, 2922 cm^{-1}.

General Procedure for the Preparation of Compounds 17, 19, 29, and 30. *Example: 3-Methyl-1-(4-phenylthiazol-2-yl)-1H-pyrazol-5(4H)-one (17).* A solution of 2-hydrazinyl-4-phenylthiazole (0.50 g, 2.6 mmol) and ethyl acetoacetate (0.26 g, 0.3 mL, 2.6 mmol) in glacial acetic acid (5.0 mL) was heated to reflux for 3 h. After evaporation of the solvent, the residue was treated with a saturated aqueous solution of sodium hydrogen carbonate and extracted with ethyl acetate. The organic layer was washed with brine, dried, and filtered. Removal of the solvent gave a residue that was purified by column chromatography (silica gel, ethyl acetate:*n*-hexane = 2:1 as eluent) to furnish 16 (0.42 g, 62%), mp 188−192 °C (from ethanol), lit. 188−189 °C.[29]

2-(3-Bromo-5-hydroxyphenyl)-5-methyl-2,4-dihydro-3H-pyrazol-3-one (19). It was synthesized as 17, starting from 18 and ethyl acetoacetate. Yield 13%, mp 170−172 °C (from ethanol). ^1H NMR (DMSO-d_6): δ 2.06 (s, 3H), 5.35 (s, 1H), 6.73 (s, 1H), 7.23−7.35 (m, 2H), 10.04 (broad s, disappeared on treatment with D_2O, 1H), 11.72 ppm (broad s, disappeared on treatment with D_2O, 1H). IR: ν 1730, 2952, 3160 cm^{-1}.

1-(3-Hydroxy-5-(pyridin-4-yl)phenyl)-3-methyl-1H-pyrazol-5(4H)-one (29). It was synthesized as 17, starting from 27 and ethyl acetoacetate. Yield 13%, mp 250 °C with decomposition (from ethanol). ^1H NMR (DMSO-d_6): δ 2.09 (s, 3H), 5.38 (s, 1H), 6.92−6.95 (m, 1H), 7.30−7.32 (m, 1H), 7.52−7.59 (m, 3H), 8.60−8.62 (m, 2H), 9.89 (broad s, disappeared on treatment with D_2O, 1H), 11.57 ppm (broad s, disappeared on treatment with D_2O, 1H). IR: ν 1736, 2854, 2923, 2932 cm^{-1}.

1-(4′-(Dimethylamino)-[1,1′-biphenyl]-3-yl)-3-methyl-1H-pyrazol-5(4H)-one (30). It was synthesized as 17, starting from 28 and ethyl acetoacetate. Yield 12%, slurry. ^1H NMR (DMSO-d_6): δ 2.12 (s, 3H), 2.94 (s, 6H), 5.43 (s, 1H), 6.80 (d, J = 8.8 Hz, 2H), 7.39−7.41 (m, 2H), 7.49−7.53 (m, 3H), 7.87 (s, 1H), 11.51 ppm (broad s, disappeared on treatment with D_2O, 1H). IR: ν 1715, 2803, 2852, 2921 cm^{-1}.

General Procedure for the Preparation of Compounds 18, 27, and 28. *Example: 3-Bromo-5-hydrazinylphenol Hydrochloride (18).* A mixture of 3-bromo-5-nitrophenol[30] (1.0 g, 4.6 mmol) and tin(II) chloride dihydrate (5.17 g, 23 mmol) in ethyl acetate (30.0 mL) was heated to reflux for 3 h. After cooling, the reaction mixture was made basic with a saturated aqueous solution of sodium hydrogen carbonate and the resulting suspension filtered. Layers were separated and the organic one washed with brine, dried, and filtered. Removal of the solvent gave 3-amino-5-bromophenol (0.86 g) that was used without further purification. To a cold solution of crude 3-amino-5-bromophenol (0.86 g, 4.5 mmol) in 37% hydrogen chloride (9.4 mL), a solution of sodium nitrite (0.32 g, 4.6 mmol) in water (2.3 mL) was added dropwise. The reaction mixture was stirred at 0 °C for 20 min, and a solution of tin(II) chloride dihydrate (2.30 g, 10 mmol) in 37% hydrogen chloride was added dropwise. The reaction mixture was stirred at the same temperature for additional 20 min and resulting suspension filtered to give 18 (0.93 g) that was used without further purification.

3-Hydrazinyl-5-(pyridin-4-yl)phenol Hydrochloride (27). It was synthesized as 18 starting from 25 and was used without further purification.

3′-Hydrazinyl-N,N-dimethyl-[1,1′-biphenyl]-4-amine Hydrochloride (28). It was synthesized as 18 starting from 26 and was used without further purification.

Peptide Synthesis. N^{α}-Fmoc-protected amino acids, Fmoc-Rink Amide-Am resin, *O*-benzotriazole-*N*,*N*,*N*′,*N*′-tetramethyl-uronium-hexafluorophosphate (HBTU), *N*,*N*-diisopropylethylamine (DIEA), triisopropylsilane (TIS), trifluoroacetic acid (TFA), and piperidine were purchased from IRIS Biotech, *N*-hydroxybenzotriazole (HOBt), *N*,*N*-dimethylformamide (DMF), dichloromethane (DCM), and fluorescein-5-isothiocyanate (FITC) from Organics (Morris Plains). For N^{α}-Fmoc-protected amino acids, the following side chain protecting groups were used: Arg(Pbf), Asn(Trt), Asp(OtBu), Gln(Trt), Trp(N^{in}-Boc), and Tyr(*t*Bu). Solvents and reagents were reagent grade and used without further purification unless otherwise noted. Peptides were analyzed by analytical HPLC (Shimadzu Prominance HPLC system) equipped with a C18-bounded analytical reverse-phase HPLC column (Phenomenex Luna, 4.6 mm × 250 mm 5 μM) using a gradient elution (10−90% acetonitrile in water (0.1% TFA) over 20 min; flow rate = 1.0 mL/min; diode array UV detector). Peptides were purified by preparative HPLC (Shimadzu HPLC system) equipped with a C18-bounded preparative reverse-phase HPLC column (Phenomenex Kinetex 21.2 mm × 150 mm 5 μm). Molecular weights of compounds were confirmed by ESI-mass spectrometry using an Agilent 6110 quadrupole LC/MS system

Peptide syntheses were performed manually by a stepwise solid-phase procedure using 0.1 mmol Rink Amide aminomethyl-polystyrene resin (0.48 mmol/g). The linear sequence was synthesized by introducing each amino acid with the following protocols: (1) deprotection of N^{α}-Fmoc protecting group by the treatment with piperidine (20% in DMF; 1 × 5 min and 1 × 25 min), and (2) coupling reaction using Fmoc-AA (4 equiv) in the presence of HBTU (152 mg, 4 equiv), HOBt (54 mg, 4 equiv), and DIEA (140 μL, 8 equiv) in DMF (2 mL) for 2 h at room temperature. The coupling efficiency for each amino acid was determined by the quantitative ninhydrin test and TNBS test. Next, for the peptide BIM-RIF, the N^{α}-Fmoc of the last amino acid was removed and the free amino group was acetylated with acetic anhydride (96 μL, 8 equiv) and DIPEA (174 μL, 4 equiv) in DCM (4 mL) for 30 min. For FITC-BIM, once amino hexanoic acid (Ahx) was introduced as spacer, the peptide was fluorescently labeled by mixing the resin with of fluorescein-5-isothiocyanate (FITC) (238 mg, 6 equiv) and DIEA (210 μL, 12 equiv) in minimal DMF for 12 h in the dark. Finally, both the peptides were cleaved from the resin by the treatment with TFA/TIS/water (10 mL, 90:5:5) for 3 h at room temperature. Then, the resin was filtered and the TFA solution and the peptide was precipitated by adding cold diethyl ether (40 mL) and centrifuged. Crude peptide extracts were then analyzed by analytical reverse-phase HPLC. Analytical separations

were conducted in 0.1% TFA with an acetonitrile gradient (10−90% acetonitrile in water over 20 min, flow rate of 1.0 mL/min) on a Phenomenex C18 column (0.46 mm × 150 mm 5 μm). After analytical analysis, the crude peptide was purified by preparative chromatography in 0.1% TFA with an acetonitrile gradient (10−90% acetonitrile in water over 15 min, flow rate of 15 mL/min) on a Phenomenex Kinetex C18 column (21.2 mm × 150 mm 5 μm).

Acetylated-BIM (Ac-BIM) (Ac-DMRPEIWIAQELRRIGDEFNAYYARR-NH_2). Purity >95%, t_R 16.2 min (analytical HPLC, 10−90% acetonitrile in water (0.1% TFA) over 20 min, flow rate of 1.0 mL/min); molecular formula, $C_{147}H_{225}N_{45}O_{41}S$; calculated mass, 3308.7; found, 1104.4 (M + 3H)/3, 828.4 (M + 4)/4.

FITC-BIM (FITC-Ahx-EIWIAQELRRIGDEFNAYYARR-NH_2). Purity >95%, t_R 12.3 min (analytical HPLC, 10−90% acetonitrile in water (0.1% TFA) over 20 min, flow rate of 1.0 mL/min); molecular formula, $C_{152}H_{212}N_{40}O_{40}S$; calculated mass, 3269.6; found, 1090.8 (M + 3H)/3.

Molecular Modeling. Molecular docking of 1 and 8 into the solution structure of BAX (PDB code: 2K7W) was carried out using the Glide 5.5 program.[31] Maestro 9.0.211[32] was employed as the graphical user interface, and Figure 1 was rendered by the Chimera software package.[33] The inhibitor structures were first generated through the Maestro sketcher and prepared through the LigPrep module. The target protein was prepared through the Protein Preparation Wizard of the graphical user interface Maestro and the OPLS-2001 force field. Water molecules were removed, hydrogen atoms were added, and minimization was performed until the RMSD of all heavy atoms was within 0.3 Å of the crystallographically determined positions. The binding pocket was identified by placing a 20 Å cube centered on the BIM helix. Molecular docking calculations were performed with the aid of Glide 5.5 in extra-precision (XP) mode, using Glidescore for ligand ranking. For multiple ligand docking experiments, an output maximum of 5000 ligand poses per docking run with a limit of 100 poses for each ligand was adopted.

Biology. *Reagents.* Salt and organic solvents were from Fluka, Sigma-Aldrich (USA), Applichem (Germany), and Carlo Erba (Italy). FITC, Texas Red, and HRP conjugated monoclonal and polyclonal secondary antibodies were from Sigma-Aldrich (USA). The caspase inhibitor peptide NAc-Asp-Glu-Val-Asp-al (Ac-DEVD-CHO) was from Sigma. *Escherichia coli* produced recombinant *N*-terminal GST-tagged human BAX (SRP5166), Bcl-2 (SRP0186), and Bcl-XL (SRP0187) were from Sigma.

Cell Cultures. HuH7[34] cells were cultured in DMEM supplemented with 10% FBS. SHSY-5Y[35] were cultured in DMEM/F12 medium supplemented with 10% FBS and nonessential amminoacids. NB4[19] and Jurkat[36] cells were cultured in RPMI medium supplemented with 10% FBS. Lewis lung carcinoma cells (LLC1),[22] kindly gifted from Prof. Aldo Pinto (Department of Pharmaceutical and Biomedical Sciences, University of Salerno, Italy), were cultured in DMEM containing 10% FBS, penicillin (100 U/mL), and streptomycin (100 μg/mL). MEF cells wild-type (MEF wt), MEF BCL-2 knockout (MEF Bcl2$^{-/-}$), MEF BAD knockout (MEF Bad$^{-/-}$), MEF BAX knockout (MEF BAX$^{-/-}$), MEF BID knockout (MEF Bid$^{-/-}$), MEF BAK knockout (MEF Bak$^{-/-}$), and MEF BAX/BAK double knockout (MEF BAX$^{-/-}$BAK$^{-/-}$) were purchased from ATCC (TCP-2110) and grown in IMDM supplemented with 10% FBS supplemented with nonessential amminoacids and cultivated according manufacturer procedures. All cultures were grown in an atmosphere of 5% CO_2 at 37 °C.

Primary Antibodies. Polyclonal AntiBax N20 (Santa Cruz), monoclonal AntiBax 6A7 (Santa Cruz), polyclonal Anti active Casp-3 (Abgene), and polyclonal anti Cyt-C (Santa Cruz).

Buffers. Buffer B: 20 mM Tris HCl pH 7.4, NaCl 150 mM, protease inhibitors. Buffer D: 100 mM potassium phosphate pH 6.7, 7.5 mM $MgCl_2$, 250 mM sucrose, digitonin 40 μg/mL. Buffer E: 20 mM Hepes KOH pH 7.4, 150 mM NaCl. Buffer F: 3.7% formaldehyde in PBS pH 7.4. Buffer G: 0.1 M glycine in PBS. Buffer H: 20 mM Hepes KOH pH 7.4, 120 mM sucrose. Buffer S: 1% SDS in Buffer B. Buffer L: 1% Tryton X-100 in Buffer B. Buffer T: 0.1% Triton in PBS pH 7.4.

Fluorescence Polarization Binding Assay. FITC-BIM direct binding curves to GST-BAX, BCL-2, and BCL-XL were generated by incubation of the fluorescent peptide (50 nM) with the indicated dilution of recombinant purified proteins in buffer E. Fluorescent polarization was measured before and after the addition of Acetylated-BIM (50 μM). FITC-BIM specific binding was calculated subtracting nonspecific binding (measured in the presence of Acetylated-BIM) from total binding (measured in the absence of acetylated-BIM). EC_{50} was calculated by fitting direct total binding data by nonlinear regression analysis of dose−response curve using Prism software (GraphPad). K_i was calculated by fitting direct specific binding data by nonlinear regression analysis of competitive binding curves. Fluorescent polarization was measured with an Envision station (PerkinElmer) using the following setting (excitation filter, FITC-FP-480 (code: 104) (X480; CWL = 480 nm; BW = 30 nm; T_{min} = 70%); emission filter (P), FITC FP P-pol 535 (code: 209) (M535p; CWL = 535 nm; BW = 40 nm; T_{min} = 80%); emission filter (S) FITC FP S-pol 535 (code: 208) (M535s; CWL = 535 nm; BW = 40 nm; T_{min} = 80%) and the mirror modules FP 431 used by top. For competition assays, serial dilution of the candidate compounds were obtained by dilution in buffer E supplemented with 50 nM FITC-BIM. After 5 min, recombinant proteins were added to the mixture at 1 μM concentration. Fluorescence polarization was measured after 30 min of incubation. Measurements were done in triplicates, and pK_i were calculated fitting the values by nonlinear regression analysis of competitive binding curves using Prism software (GraphPad). All the best-fit values reported in Table 1 had SE <10% (the curve fitting for competitive binding of compound 3 to BAX has SE <15%, the one of compound 15 for Bcl-2 has SE <16%).

Assessment of Apoptosis Rate. Mother stocks of compounds dissolved in DMSO (30 mM) were diluted in complete culture medium. Cells were treated with the diluted compounds for the indicated time. After treatment, cells were fixed in buffer F and apoptosis rate was measured by evaluation of nuclear fragmentation (visualized by DAPI staining), positivity to antiactive caspase 3 antibody, and blebbing of cell membrane. Percent of cells in apoptosis was calculated by counting cells from 20 random fields. Measurements were done in triplicate, and EC_{50} were calculated fitting the values by nonlinear regression analysis of competitive binding curves using Prism software (GraphPad). All the best-fit values reported in Table 1 had SE <10%.

Immunofluorescence. HuH7 cells growing on glass coverslips were fixed in buffer F for 30 min. Formaldehyde was quenched by incubating the coverslips for 30 min in buffer G. Cells were permeabilized in buffer T for 10 min at 25 °C to then be incubated with primary and secondary antibody diluted in PBS for 1 h and 30 min, respectively. The following dilutions were used: polyclonal anti-Bax 1:50, antiactive Casp-3 1:500, DAPI 1:400, and anti Cyt-C 1:200. Immunofluorescence images were taken by a Leica DFC320 video camera (Leica, Milan, Italy) connected to a Leica DMRB microscope equipped with a 100× objective, and the ImageJ Software (National Institutes of Health, Bethesda, MD) was used for analysis.

MitoTracker Staining and Measurement. Cells were incubated for 30 min at 37 °C in complete medium supplemented with MitoTracker Red CMXRos (Invitrogen) at the final concentration of 200 nM. After the incubation, cells were washed twice in fresh medium and then lysed in absolute DMSO. The absorbance of the probe was read at 570 nM in a spectrophotometer. For microscope visualization of stained cells, cells were fixed in buffer F and processed as described above.

Mice. Female C57BL/6J mice (6 wks) were purchased from Harlan Laboratories (Milan, Italy) and housed at the Department of Pharmacy, University of Naples, Italy. Before the experiments, the mice were acclimated for 1 week and were fed with standard chow diet and water ad libitum. All animal experiments were performed under protocols that followed the Italian and European Community Council for Animal Care (DL no. 116/92).

Animal Experiments. Subconfluent LLC1 cells were harvested and passed through a 40 μm cell strainer, washed 3 times in PBS, resuspended in PBS, and inoculated at 3 × 10^5 cells in 7 week old mice through the tail vein (day 0). After 14 days, mice were randomly

divided into two groups: control and 8 1 mg/kg (n = 6 and n = 8, respectively). For the treatment, 8 was first dissolved in DMSO and then suspended in sterile water (1% DMSO final concentration). 8 (1 mg/kg) was administered once a day by ip injection from day 14 to 17. The control group received 1% DMSO (2 μL) daily. At day 18, mice were euthanized, the thorax was opened, and the lungs were perfused with phosphate-buffered saline (PBS), pH 7.4, via the pulmonary artery to remove blood. The entire tumor-bearing lung was used and examined as described below. Drug toxicity indexes such as weight loss, ruffled fur, behavior change, and feeding patterns were continuously observed during the whole treatment.

Splenocyte Preparation. C57BL/6J mice were euthanized as already described. After excision, spleen was sliced into pieces and passed through a strainer using the plunger end of a syringe. Cell suspension was centrifuged for 5 min at 1600 rpm and cell pellet resuspended in prewarmed complete culture medium with the treatment with compounds starting immediately.

Organic Extraction of Tissue. First, 100 μg of protein lysates were supplemented with 9 volumes of cold acetone and incubated for 2 h at −20 °C. Proteins were then pelleted by centrifuging the samples at 14000 rpm at 4 °C. The absorbance spectrum of the organic extracts (1 mL in volume using quartz cuvettes) was recorded in the wavelength range between 220 and 800 nM and compared with the absorbance spectra of 8 10 μM in water, acetone, or extraction buffer (acetone:water = 9:1) as indicated.

Histological Analysis. Right lung lobes were fixed in 10% buffered formalin for 24−48 h. The fixed lobes were cut in two transverse portions, paraffin-embedded, and sectioned at 7 μm. Haematoxylin and eosin staining was performed and used to measure the tumor burden. Tumor lesions and lung area were analyzed by using 20 serial sections per lobe. The results were expressed as the ratio of the tumor lesions area compared with the total lung area. Images were taken by a Leica DFC320 video camera (Leica, Milan, Italy) connected to a Leica DMRB microscope, and the ImageJ Software (National Institutes of Health, Bethesda, MD) was used for analysis.

Mitochondria Isolation. Cells or lung tissue were incubated in buffer D for 30 min. After lysis, cell debris and permeabilized cells were spun down for 30 min at 3000*g* (4 °C). Mitochondrial fractions were obtained centrifuging the supernatant for 30 min at 14000*g*. Mitochondrial pellet was lysed in B-buffer 1% Triton for 1 h at 4 °C.

Processing of the Tissues. Lung tissues were disrupted in buffer H in a Teflon Douce. The tissue homogenate was supplemented with 1% Triton and incubated for 1 h on ice. Cell debris and unbroken cells were sedimented by spinning down the homogenate for 1 h at 14000*g*. The supernatant containing the protein extracts was quantitated by Biorad (Pierce) using BSA as standard. Equal amounts of protein were processed further and stored at −80 °C after having been snap frozen in liquid nitrogen.

Immunoprecipitation. Lysates were immunoprecipitated with 6A7 anti-BAX mouse monoclonal antibody overnight at 4 °C (25 μL of antibody per mL of lysate) and with protein-A sepharose for 45 min followed by fur washes in buffer L. After the last wash, beads were resuspended in 20 μL of buffer L before Western blot processing.

Western Blotting. Samples were diluted in 20 mM Tris HCl (pH 6.8), 50 mM DTT, 1% SDS, 5% glycerol, and bromophenol blue to then be boiled for 10 min at 95 °C. Samples were loaded on a 12.5% SDS PAGE gel. Run was performed at 100 V at 25 °C. After the run, proteins were transferred on nitrocellulose filter (Schleicher-Schuel) at 80 V for 1 h at 4 °C. Filters were blocked for 2 h at 25 °C in PBS supplemented with 3% nonfat dry milk (Biorad) for 2 h at 25 °C and incubated with primary and secondary antibody diluted in PBS supplemented with 0.3% nonfat dry milk in PBS. ECL reaction was performed using the Lumi Light ECL kit (Roche) according manufacturer procedures.

AUTHOR INFORMATION

Corresponding Authors

*For M.S.: E-mail, mariano.stornaiuolo@gmail.com.

*For L.M.: phone, 0039-328-6795645; E-mail, lmarinel@unina.it.

Author Contributions

The manuscript was written through contributions of all authors. All authors have given approval to the final version of the manuscript.

Notes

The authors declare no competing financial interest.

ACKNOWLEDGMENTS

The research program was funded by FIRB-Programma "Futuro in Ricerca" RBFR10ZJQT. We thank Alessia Ciogli for HRMS spectral analyses.

ABBREVIATIONS USED

MOMP, mitochondrial outer membrane permeabilization; GST, glutatione S-transferase; FITC, fluorescein isothiocyanate; MEF, mouse embryonic fibroblasts

REFERENCES

(1) Bodur, C.; Basaga, H. Bcl-2 inhibitors: emerging drugs in cancer therapy. *Curr. Med. Chem.* 2012, *19*, 1804−1820.

(2) Tait, S. W.; Green, D. R. Mitochondria and cell death: outer membrane permeabilization and beyond. *Nature Rev. Mol. Cell Biol.* 2012, *11*, 621−632.

(3) Green, D. R.; Walczak, H. Apoptosis therapy: driving cancers down the road to ruin. *Nature Med.* 2013, *19*, 131−133.

(4) Zong, W.-X.; Cheng, E. H.-Y.; Lindsten, T.; Panoutsakopoulou, V.; Ross, A. J.; Roth, K. A.; MacGregor, G. R.; Thompson, C. B.; Korsmeyer, S. J. BAX and BAK: a requisite gateway to mitochondrial dysfunction and death. *Science* 2001, *292*, 727−730.

(5) Du, H.; Wolf, J.; Schafer, B.; Moldoveanu, T.; Chipuk, J. E.; Kuwana, T. BH3 domains other than Bim and Bid can directly activate Bax/Bak. *J. Biol. Chem.* 2011, *286*, 491−501.

(6) Ni Chonghaile, T.; Letai, A. Mimicking the BH3 domain to kill cancer cells. *Oncogene* 2008, *27*, 149−157.

(7) Oltersdorf, T.; Elmore, S. W.; Shoemaker, A. R.; Armstrong, R. C.; Augeri, D. J.; Belli, B. A.; Bruncko, M.; Deckwerth, T. L.; Dinges, J.; Hajduk, P. J.; Joseph, M. K.; Kitada, S.; Korsmeyer, S. J.; Kunzer, A. R.; Letai, A.; Li, C.; Mitten, M. J.; Nettesheim, D. G.; Ng, S.; Nimmer, P. M.; O'Connor, J. M.; Oleksijew, A.; Petros, A. M.; Reed, J. C.; Shen, W.; Tahir, S. K.; Thompson, C. B.; Tomaselli, K. J.; Wang, B.; Wendt, M. D.; Zhang, H.; Fesik, S. W.; Rosenberg, S. H. An inhibitor of Bcl-2 family proteins induces regression of solid tumours. *Nature* 2005, *435*, 677−681.

(8) Tse, C.; Shoemaker, A. R.; Adickes, J.; Anderson, M. G.; Chen, J.; Jin, S.; Johnson, E. F.; Marsh, K. C.; Mitten, M. J.; Nimmer, P.; Roberts, L.; Tahir, S. K.; Xiao, Y.; Yang, X.; Zhang, H.; Fesik, S.; Rosenberg, S. H.; Elmore, S. W. ABT-263: a potent and orally bioavailable Bcl-2 family inhibitor. *Cancer Res.* 2008, *68*, 3421−3428.

(9) Souers, A. J.; Leverson, J. D.; Boghaert, E. R.; Ackler, S. L.; Catron, N. D.; Chen, J.; Dayton, B. D.; Ding, H.; Enschede, S. H.; Fairbrother, W. J.; Huang, D. C.; Hymowitz, S. G.; Jin, S.; Khaw, S. L.; Kovar, P. J.; Lam, L. T.; Lee, J.; Maecker, H. L.; Marsh, K. C.; Mason, K. D.; Mitten, M. J.; Nimmer, P. M.; Oleksijew, A.; Park, C. H.; Park, C. M.; Phillips, D. C.; Roberts, A. W.; Sampath, D.; Seymour, J. F.;

Smith, M. L.; Sullivan, G. M.; Tahir, S. K.; Tse, C.; Wendt, M. D.; Xiao, Y.; Xue, J. C.; Zhang, H.; Humerickhouse, R. A.; Rosenberg, S. H.; Elmore, S. W. ABT-199, a potent and selective BCL-2 inhibitor, achieves antitumor activity while sparing platelets. *Nature Med.* 2013, *19*, 202−208.

(10) *ClinicalTrials.gov*; U.S. National Institutes of Health: Bethesda, MD; https://clinicaltrials.gov/ct2/results?term=ABT199&Search=Search (accessed February 4, 2015).

(11) Gavathiotis, E.; Suzuki, M.; Davis, M. L.; Pitter, K.; Bird, G. H.; Katz, S. G.; Tu, H. C.; Kim, H.; Cheng, E. H.; Tjandra, N.; Walensky, L. D. BAX activation is initiated at a novel interaction site. *Nature* 2008, *455*, 1076−1081.

(12) Gavathiotis, E.; Reyna, D. E.; Bellairs, J. A.; Leshchiner, E. S.; Walensky, L. D. Direct and selective small-molecule activation of proapoptotic BAX. *Nature Chem. Biol.* 2012, *8*, 639−645.

(13) Suzuki, M.; Youle, R. J.; Tjandra, N. Structure of BAX: coregulation of dimer formation and intracellular localization. *Cell* 2000, *103*, 645−654.

(14) Friesner, R. A.; Banks, J. L.; Murphy, R. B.; Halgren, T. A.; Klicic, J. J.; Mainz, D. T.; Repasky, M. P.; Knoll, E. H.; Shelley, M.; Perry, J. K.; Shaw, D. E.; Francis, P.; Shenkin, P. S. Glide: A new approach for rapid, accurate docking and scoring. 1. Method and assessment of docking accuracy. *J. Med. Chem.* 2004, *47*, 1739−1749.

(15) Friesner, R. A.; Murphy, R. B.; Repasky, M. P.; Frye, L. L.; Greenwood, J. R.; Halgren, T. A.; Sanschagrin, P. C.; Mainz, D. T. Extra precision Glide: docking and scoring incorporating a model of hydrophobic enclosure for protein−ligand complexes. *J. Med. Chem.* 2006, *49*, 6177−6196.

(16) Garcia-Calvo, M.; Peterson, E. P.; Leiting, B.; Ruel, R.; Nicholson, D. W.; Thornberry, N. A. Inhibition of human caspases by peptide-based and macromolecular inhibitors. *J. Biol. Chem.* 1998, *273*, 32608−32613.

(17) Cam, L.; Boucquey, A.; Coulomb-L'Hermine, A.; Weber, A.; Horellou, P. Gene transfer of constitutively active caspase-3 induces apoptosis in a human hepatoma cell line. *J. Gene Med.* 2005, *7*, 30−38.

(18) Varadarajan, S.; Vogler, M.; Butterworth, M.; Dinsdale, D.; Walensky, L. D.; Cohen, G. M. Evaluation and critical assessment of putative MCL-1 inhibitors. *Cell Death Differ.* 2013, *20*, 1475−1484.

(19) Lanotte, M.; Martin-Thouvenin, V.; Najman, S.; Balerini, P.; Valensi, F.; Berger, R. NB4, a maturation inducible cell line with t(15;17) marker isolated from a human acute promyelocytic leukemia (M3). *Blood* 1991, *77*, 1080−1086.

(20) Fruman, D. A.; Rommel, C. PI3K and cancer: lessons, challenges and opportunities. *Nature Rev. Drug Discovery* 2014, *13*, 140−156.

(21) Ovejera, A. A.; Johnson, R. K.; Goldin, A. Growth characteristics and chemotherapeutic response of intravenously implanted Lewis lung carcinoma. *Cancer Chemother. Rep.* 1975, *5*, 111−125.

(22) Brodt, P. Characterization of two highly metastatic variants of Lewis lung carcinoma with different organ specificities. *Cancer Res.* 1986, *46*, 2442−2448.

(23) Giraldi, T.; Sava, G.; Cuman, R.; Nisi, C.; Tassiani, L. Selectivity of the antimetastatic and cytotoxic effects of 1-*p*-(3,3-dimethyl-1-triazeno)benzoic acid potassium salt, (±)-1,2-di(3,5-dioxopiperazin-1-yl)propane, and cyclophosphamide in mice bearing lewis lung carcinoma. *Cancer Res.* 1981, *41*, 2524−2528.

(24) Tsuruo, T.; Iida, H.; Tsukagoshi, S.; Sakurai, Y. 4′-*O*-Tetrahydropyranyladriamycin as a potential new antitumor agent. *Cancer Res.* 1982, *42*, 1462−1467.

(25) Lv, P. C.; Xiao, Z.-P.; Fang, R.-Q.; Li, H.-Q.; Zhu, H.-L.; Liu, C.-H. Synthesis, characterization and structure−activity relationship analysis of novel depsides as potential antibacterials. *Eur. J. Med. Chem.* 2009, *44*, 1779−1787.

(26) Pschorr, R.; Zeidler, F. Morphine Series. V. Synthesis of the 3,4-Dimethoxy-8-ethoxyphenanthrene Obtained in the Degradation of Thebenine. *Justus Liebig's Ann. Chem.* 1910, *373*, 75−79.

(27) Brooks, C. A.; Cheung, M.; Eidam, H. S.; Fox, R. M.; Hilfker, M. A.; Manas, E. S.; Ye, G. 4-Quinolinecarboxamide derivatives as TRPV4 antagonists and their preparation and use for the treatment of diseases. PCT Int. Appl. WO 2011119704 A1, September 29, 2011.

(28) Bondock, S.; El-Azap, H.; Kandeel, E.-E. M.; Metwally, M. A. Eco-friendly solvent-free synthesis of thiazolylpyrazole derivatives. *Monatsh. Chem.* 2008, *139*, 1329−1335.

(29) Brooks, C. A.; Cheung, M.; Eidam, H. S.; Fox, R. M.; Hilfker, M. A.; Manas, E. S.; Ye, G. 4-Quinolinecarboxamide derivatives as TRPV4 antagonists and their preparation and use for the treatment of diseases. PCT Int. Appl. WO 2011119704 A1, September 29, 2011.

(30) Weidlich, T.; Pokorny, M.; Padelkova, Z.; Ruzicka, A. Aryl ethyl ethers prepared by ethylation using diethyl carbonate. *Green Chem. Lett. Rev.* 2007, *1*, 53−59.

(31) *Glide*, version 5.5; Schrödinger, LLC: New York, 2009.

(32) *Maestro*, version 9.0.211; Schrodinger, LLC: New York, 2009.

(33) Pettersen, E. F.; Goddard, T. D.; Huang, C. C.; Couch, G. S.; Greenblatt, D. M.; Meng, E. C.; Ferrin, T. E. UCSF Chimera□a visualization system for exploratory research and analysis. *J. Comput. Chem.* 2004, *25*, 1605−1612.

(34) Lemma, V.; D'Agostino, M.; Caporaso, M. G.; Mallardo, M.; Oliviero, G.; Stornaiuolo, M.; Bonatti, S. A disorder-to-order structural transition in the COOH-tail of Fz4 determines misfolding of the L501fsX533-Fz4 mutant. *Sci. Rep.* 2013, *3*, 2659.

(35) Biedler, J. L.; Roffler-Tarlov, S.; Schachner, M.; Freedman, L. S. Multiple neurotransmitter synthesis by human neuroblastoma cell lines and clones. *Cancer Res.* 1978, *38*, 3751−3757.

(36) Weiss, A.; Wiskocil, R. L.; Stobo, J. D. The role of T3 surface molecules in the activation of human T cells: a two-stimulus requirement for IL-2 production reflects events occurring at a pre-translational level. *J. Immunol.* 1984, *133*, 123−128.